Division 6 – Lincoln Laboratory
Massachusetts Institute of Technology
Lexington 73, Massachusetts

SUBJECT: THE INFLUENCE OF CHEMISTRY ON B-H LOOP SHAPE, COERCIVITY, AND FLUX-REVERSAL TIME IN FERRITES.
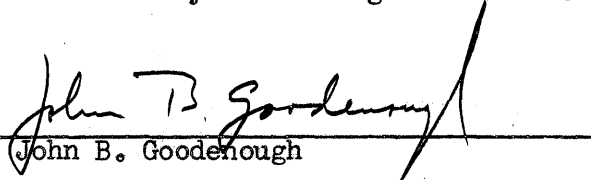
To: Group 63, Staff

From: John B. Goodenough

Date: May 16, 1956

Approved: *[signature]*

David R. Brown

Abstract: The factors which influence the shape of the B-H loop, the coercivity, the permeability, and the flux-reversal time in ferrimagnetic spinels are considered on two levels: a macroscopic and an atomic level. To minimize consideration of shape-dependent properties, the ferrite components are assumed to be toroids. With the assumption that domain walls are present in the material, the influence of grain-boundary magnetic poles on B-H loop shape, coercivity, permeability and flux reversal is determined in terms of measurable physical parameters of the material. From these relationships it is possible for the designing engineer to determine the optimum parameter values for a given application. The spinel-like magnetic oxides may, in first approximation, be considered ionic lattices. In order to obtain some insight into the control of the macroscopically measurable physical parameters by chemical composition and preparation procedures, as a second approximation the directional character of the ionic orbitals is emphasized to describe the influence of covalent effects on magnetic moment, magnetic exchange, and crystalline anisotropy. These effects are applied theoretically to the cations of particular interest in ferrites. Finally, some properties of several ferrites are displayed graphically to illustrate the importance of processing and chemistry on the magnetic character of ferrospinels.

JBG/md

[signature]
John B. Goodenough

Distribution: All of Group 63 staff to receive abstracts only.

Note: This paper is to be presented at the Convention on Ferrites, London, England, October, 1956. Copies may be obtained from Mrs. Muriel Durso, B-181

The Influence of Chemistry on B-H Loop Shape, Coercivity, and

Flux-Reversal Time in Ferrites[†]

by

John B. Goodenough, Ph.D.

Staff Member
Lincoln Laboratory
Massachusetts Institute of Technology
Lexington, Massachusetts

List of Symbols

I_s = saturation magnetization $[\text{e.m.u.}]$,

B = flux density (B_s saturation, B_r remanence, B_m at maximum applied field, B_d disturb flux density) $[\text{gauss}]$.

H = applied field strength (H_c coercivity, H_m maximum, H_{wi} critical for irreversible motion of ith wall, H_{ni} critical for creation of ith domain. H_o = average thereshold for irreversible wall motion). $[\text{oe}]$

T_c = Curie temperature $\left[^{o}K \text{ or } ^{o}C \right]$.

$A \propto T_c$ = exchange constant $[\text{ergs/cm}]$.

K = anisotropy constant $[\text{ergs/cm}^3]$ (K' effective: $E_{k'} = K' \sin^2 \phi$; K_1 first-order crystalline for cubic symmetry: $E_k = K_1(\alpha_1^2 \alpha_2^2 + \alpha_2^2 \alpha_3^2 + \alpha_3^2 \alpha_1^2)$).

σ_w = domain-wall energy per unit area $\left[\text{ergs/cm}^2 \right]$.

δ = domain-wall width $[\text{cm}]$.

v' = fractional volume of closure domains.

v = fractional volume of reverse domains.

Θ = angle between $\underline{I}_s$ and $\underline{H}$. ($\Theta = \Theta_m$ at $H = H_m$).

ω^* = $I_s(\cos\Theta_1 - \cos\Theta_2)$ is surface magnetic-pole density at a grain boundary. $[\text{e.m.u.}]$

λ = ratio of minor to major axis of a reverse domain.

L = mean grain size $[\text{cm}]$.

P = percentage of granular inclusion in lattice.

μ = permeability (μ_r = rotational, μ_w = wall contribution; μ_o = initial, μ_Δ = incremental at $B = B_r$).

t_r = rise-time of square-wave input pulse $[\text{sec}]$.

τ = flux-reversal time (duration output voltage > 0.1 peak output voltage). $[\text{sec}]$

d = distance wall moving with average velocity moves in a time τ. $[\text{cm}]$

β = viscous-damping parameter of a domain wall (β_e eddy-current, β_r relaxation contribution). $[\text{erg-sec/cm}^4]$

γ = magnetomechanical ratio $[\text{e.m.u.}]$

Λ = intrinsic relaxation frequency defined by Landau-Lifshitz equation $[\text{sec}^{-1}]$

S_w = switching coefficient defined by Eq. (18) $[\text{oe.-sec}]$.

$_uV_1$ = maximum output voltage from a core storing an undisturbed "one". $[\text{volts}]$

S_v = voltage switching parameter defined by Eq.(20) $[\text{volts/oe.}]$

The Influence of Chemistry on B-H Loop Shape, Coercivity, and

Flux-Reversal Time in Ferrites

by

John B. Goodenough, Ph.D.

Summary: The factors which influence the shape of the B-H loop, the

coercivity, the permeability, and the flux-reversal time in

ferrimagnetic spinels are considered on two levels: a macro-

scopic and an atomic level. To minimize consideration of shape-

dependent properties, the ferrite components are assumed to be

toroids. With the assumption that domain walls are present in

the material, the influence of grain-boundary magnetic poles on

B-H loop shape, coercivity, permeability and flux reversal is

determined in terms of measurable physical parameters of the

material. From these relationships it is possible for the

designing engineer to determine the optimum parameter values for

a given application. The spinel-like magnetic oxides may, in

first approximation, be considered ionic lattices. In order to

obtain some insight into the control of the macroscopically

measurable physical parameters by chemical composition and

preparation procedures, as a second approximation the direc-

tional character of the ionic orbitals is emphasized to describe

the influence of covalent effects on magnetic moment, magnetic

exchange, and crystalline anisotropy. These effects are applied

theoretically to the cations of particular interest in ferrites.

Finally, some properties of several ferrites are displayed

graphically to illustrate the importance of processing and

chemistry on the magnetic character of ferrospinels.

(1) Introduction

The engineer needs to know the limiting values he can expect
for the basic design parameters of any circuit component; in the case
of magnetic cores for magnetic circuitry he is interested in the shape
and size of the B-H loop, the initial permeability, the pulse incremental
permeability at remanence, the relationship between driving field and
flux-reversal time, and the energy loss per flux-reversal cycle. In this
paper these design parameters are expressed in terms of measurable physi-
cal parameters of ferromagnetic materials. A discussion of the effect of
component shape is minimized; all components are assumed to be toroids.

The manufacturer who is responsible for supplying a particular
component which will meet the specifications of the design engineer within
narrow tolerances needs to know the influence of chemistry and processing
procedures on the measurable physical parameters which determine the
specified design parameters. In the third section of this paper a chemi-
cal model is suggested which, it is hoped, may serve as a guide for the
component engineer who wishes to design some new ferrite for a specific
job. This model is qualitative; yet it has the advantage of being
easily visualized and has had encouraging success in correlating observa-
tions of cation distribution, lattice distortion from close-packed
symmetry, and magnetic-exchange interactions in several magnetic oxides.

(2) Macroscopic Considerations
(2.1) Preliminary Models

In order to obtain expressions for the macroscopic parameters
or properties of ferrites in terms of fundamental, measurable parameters,
it is first necessary to have a model of magnetism and of the mechanisms
of flux change. The ferrites have a spinel-type lattice which consists

of a cubic-close-packed lattice of oxygen ions with cations located in both tetrahedral and octahedral interstices. In the unit cell there are 32 oxygen ions, 16 octahedral-site cations, and 8 tetrahedral-site cations. The magnetism of the ferrites originates with the atomic moments associated with cations which have a partially filled d shell. Not all of the cations have a net magnetic moment. As in the ferromagnetic metals, below a critical temperature, the Curie temperature, the individual atomic moments become ordered. Whereas the order in ferromagnetic crystals is a parallel alignment of the individual moments over large regions, or domains, of the lattice, in the usual ferrites[*] the tetrahedral-site magnetic moments order parallel to one another and antiparallel to the octahedral-site moments. If the net moment on the two sets of sites are of unequal magnitude, the domains carry a net macroscopic magnetic moment; because of the antiferromagnetic coupling of the cations on different types of sites, the ferrites are called ferrimagnetic rather than ferromagnetic. However, the macroscopic properties of the ferrimagnetic spinels are equivalent to those of a ferromagnetic material of low flux density.

The fundamental parameters in terms of which the macroscopic properties common to both ferromagnetic and ferrimagnetic materials may be expressed are: the Curie temperature, the spontaneous magnetization, the magnetostriction constants, the anisotropy constants, the elastic constants, the electrical resistivity, and the magneto-mechanical ratio.

There are three factors which contribute to the crystalline anisotropy: crystalline-bonding energy which is maximized if the magnetization is along a "preferred" crystal direction in the lattice, shape-dependent

---

[*] For the theory of magnetic ordering in spinels, see refs. (1),(2).
For a discussion of the experimental verification of these theories, see refs. (3)-(6) .

demagnetization energies which tend to be minimized, and magnetostriction which is sensitive to any anisotropy in the strain energy such as might be induced by a tensile or compressive stress. In the ferrimagnetic materials the resistivity can vary from 4×10^{-3} ohm-cm for magnetite[7] to 10^{11} ohm-cm for high-resistivity $MgFe_2O_4$.

Besides these common properties, both ferro- and ferrimagnetic materials in the demagnetized state are usually composed of many regions of ordered magnetic moments, the magnetic domains, of varying size and orientation. The transition region between any two domains is known as a domain wall. Through this transition region the atomic moments rotate (where possible) about an axis normal to the wall to eliminate (or minimize) free magnetic poles. In terms of the fundamental parameters of the material, the domain-wall width δ and the domain-wall energy per unit area σ_w are given by[*]

$$\delta \approx 7(A/K')^{1/2}; \quad \sigma_w = a(K'A)^{1/2} \tag{1}$$

where K' is the effective anisotropy constant in ergs/cm^3, the energy required to rotate the magnetization a small angle ϕ from an easy-magnetization direction being $K'\sin^2\phi$. The parameter A is known as the exchange constant; it measures the strength of the long-range interaction between atomic magnetic moments and is therefore proportional to the Curie temperature T_c. In a cubic crystal the proportionality constant a varies between 2 and 4 depending upon the curvature of the wall.

The number and shape of the magnetic domains within a crystal are determined by the structure of the body and its magnetic history. Since there is energy associated with a domain wall, such a wall is created only if some other energy term is correspondingly reduced. If a square

[*] For a review article on domain theory, see ref. (8).

block of material is saturated, there is a large amount of energy associated with the demagnetizing fields. This energy can be reduced by the creation of many domains of alternating polarity.* If there is an axis of easy magnetization nearly parallel to the surface of the crystal with large free-pole density, this energy can be still further reduced by the creation at that surface of closure domains which serve to close the flux path within the material.

In a toroidal specimen of cubic crystal symmetry there are no external surfaces which are perpendicular to the magnetization, and demagnetizing fields are minimized. In nonoriented polycrystalline samples, however, magnetic poles and associated demagnetizing-field energies are not completely eliminated. In fact there are two kinds of surfaces at which magnetic poles exist, the bounding surfaces of the material and the grain boundaries. The demagnetizing fields associated with these poles may be of sufficient magnitude to create new domains, the demagnetization energy being reduced at the expense of new domain-wall energy. The new walls may surround either reverse or closure domains. Closure domains are usually formed at granular inclusions, reverse domains at grain boundaries or lamellar precipitates. Either closure or reverse domains may be formed at the external surfaces depending upon the angle the magnetization vector makes with the surface. The surface magnetic-pole density at a grain boundary is $\omega^* = I_s(\cos\Theta_1 - \cos\Theta_2)$, where Θ_1, Θ_2 are the angles the grain-boundary normal makes with the magnetization vectors in the two adjacent grains. If grain-boundary precipitates or inhomogeneities from grain-to-grain exist, this surface pole density is substantially increased.

The magnetization in a toroidal component may reverse its direction by either of two mechanisms, domain rotation or reverse-domain

---

* For a discussion of domain patterns to be anticipated on surfaces perpendicular to the magnetization direction in permanent magnets, see ref (9).

creation and/or domain-wall motion. Although the primary contribution to the initial permeability in porous, fine-grained materials with small anisotropy may be domain rotation, the primary major-loop flux-reversal mechanism in a toroid is domain-wall creation and/or motion. Further, the domain walls of interest for flux reversal are the mobile walls: walls which are practically immobile in the driving fields applied to the magnetic toroid during use do not contribute significantly to the output voltage. Recently domain patterns have been observed with colloidal magnetite on surfaces of polycrystalline magnesium-manganese ferrites.[*]

The discussions to follow of flux reversal and incremental permeability at remanence are based on a model in which the mobile domain walls responsible for flux reversal are created at grain boundaries.[§] These domain walls are assumed to be 180° walls surrounding an ellipsoidal domain of reverse magnetization of eccentricity $(1 - \chi^2)^{1/2}$. In the presence of a driving field, these ellipsoidal domains grow by extending into cylinders and expanding radially until they collide with other growing domains, the colliding walls annihilating each other. The properties of ferrites driven at such high frequencies that little domain-wall motion occurs ($>$100-megacycle frequencies) are not discussed.

(2.2) The Shape of the B-H Loop

The shape of the B-H loop under operating conditions is important for many applications. If this shape is to be controlled, it

---

[*] This work was done by F. S. Maddocks of the Lincoln Laboratory and is recorded on film.

[§] Bates and Martin[37] have recently demonstrated by colloidal-magnetite techniques on silicon-iron samples that a reverse domain is created at an inclusion large enough to support closure domains if a 90° wall moves past it. If few mobile 90° walls are present, this mechanism for reverse-domain creation is probably not the dominant one. Further, this mechanism for reverse-domain nucleation would be less sensitive to external stress than grain-boundary nucleation (See Eqs.(3),(8); ref(10); Figs. 4, 6).

is necessary to understand the factors which influence it. It can be described by four parameters, the maximum flux density B_m, the retentivity B_r, the disturb flux density B_d, and the coercivity H_c. These terms are all defined in Fig. 1. The squareness ratio $R_s \equiv B_d/B_m$ is usually more meaningful than B_d itself. The flux density B in a toroid may be expressed as

$$B = H + 4\pi I_s(1 - v' - 2v) \langle \cos \Theta \rangle , \qquad (2)$$

where v', v are, respectively, the fractional volumes of closure and reverse domains and $\langle \cos \Theta \rangle$ is the average field-direction component of the spontaneous magnetization in the various crystallites, or grains. The quantities v', v, Θ depend upon the applied field strength H; however, their H dependence varies from material to material and is also structure sensitive. At saturation $B = B_s$ and $v' = v = \Theta = 0$. In toroids of soft magnetic material which are driven by soft magnetic fields ($|H_m| < 5$ oe), variations with H in v' are probably small and do not contribute appreciably to the flux change. The principal contribution to the flux change with changing field strength comes from variations in v. Only if $H_m/H_c(\text{sat.}) \ll 1$ may variations in Θ make a dominant contribution.

It was pointed out above that as H is reduced from saturation, the domains contributing to v' and v are created at surfaces of high surface magnetic-pole density. The field strength at which the ith such domain is created is defined as H_{ni}. It is defined as positive if the new reverse domain has a positive component in its direction. Further, if the walls bounding such a domain only move reversibly with a change of field strength, the wall motion is small and contributes little flux change. These reversible motions are important for initial or incremental permeability. However, the significant wall motions for flux reversal

-7-

are irreversible. The field strength required for an irreversible motion of the domain wall surrounding the ith domain contributing to v' or v is defined as H_{wi}. It is defined as positive if the growing domain has a positive component in its direction.

The important features determining the shape of the B-H loop are therefore the value of the spontaneous magnetization I_s, the various critical field strengths for new-domain creation H_{ni}, and the critical field strengths for irreversible wall motion H_{wi}. Contributions from domain rotation, or changes in Θ with H, are usually smaller unless the variations in H are too small for significant wall motion or creation to occur. In small-grained, porous ferrites rotation can dominate the initial-permeability loop. In ferrites I_s is always relatively low, but with suitable chemistry to alter the balance of magnetic moments on the two competing sets of sites, $4\pi I_s$ may be varied at room temperature from zero to over 6000 gauss.*

It is reasonable to assume that the domains contributing to v' and v which originate at the bounding surfaces of the material are practically immobile over ordinary operating fields. Their existence plus the finite angle $\Theta = \Theta_m$ at $H = H_m$ makes $B_m < B_s$; otherwise they have little effect on the shape of the B-H loop. If there are lamellar or grain-boundary precipitates present, there may be a large internal area bounding the material; in such a case a large percentage of the flux reversal may be due to the creation of reverse domains, the movement of walls over the surfaces of high pole density being quite small. Then the loop has low retentivity and large coercivity since the majority of

---

* In some spinel-type lattices the net magnetization is due to one set of sites at high temperatures and to another at low temperatures, the variation of the spontaneous magnetization with temperature in the two sets of sites being different. See refs (1),(4),(6).

$H_{ni} < 0$ and the H_{wi} are large. If low coercivity, high retentivity
materials are desired, lamellar or grain-boundary precipitates must be
avoided. The effects of those precipitates on the magnesium-manganese
ferrite system are illustrated in Fig. 2 where contours of maximum
squareness ratio are plotted against composition.

Similarly porous materials have large internal bounding surfaces
which will act as centers for domain creation with $H_{ni} < 0$ if the radius
of the inclusions are greater than a domain-wall width δ. The re-
tentivity is correspondingly reduced. The domains at these inclusions
may be considered immobile; however, they and the small inclusions which
do not support closure or reverse domains interact with the mobile domain
walls to considerably increase the coercivity. The explicit expression
for this interaction is given in Eq. (6) below. Therefore the retentivity
decreases and the coercivity increases with the porosity of the ferrite.*

In dense, single-phase toroids the reverse domains which deter-
mine the shape of the minor B-H loop defined by $- H_m \le H \le H_m$ are assumed
to be created at grain boundaries.§ In the calculation of the critical
field strength H_{ni}, it was assumed[10] that the grain boundaries are planar
and that the newly created domains are prolate ellipsoids intersecting
the planar surface periodically within an area D^2, the circle of inter-
section having a radius $r < D$ and the minor-to-major axial ratio being
$\lambda = r/\ell \ll 1$. The angles Θ_1, Θ_2 which the magnetization on either side
of the surface makes with the surface normal are assumed so small that
the demagnetization factor of the reverse domain may be taken as

---

* Data supporting these qualitative statements are given by ref (11)

§ For arguments justifying this assumption, see ref (10). More recent
experimental data is given by ref (12).

$N = 4\pi \lambda^2 \left[\ln(2/\lambda)-1\right]$, the volume as $V = 4\pi r^2 \ell /3$, and the surface area as $A_w = \pi^2 r \ell$. The critical field strength H_{ni} is taken as that which makes the free energy of the system without reverse domains at the ith surface equal to that with reverse domains. If the value of D is optimized for a given ratio $b = D/r$ and a fixed $\lambda = r/\ell$, the nucleation field strength becomes

$$H_{ni} \approx A_1 \left(A_2 \sigma_w - \omega^{*2} L\right) \tag{3}$$

with $A_1 = b^2 / \left[4 I_s \ell (\cos \alpha_1 + \cos \alpha_2)\right]$; $A_2 = 9\pi/(2b^2 \lambda) \sim 30$ in ferrites. The angles α_1, α_2 are those made by the applied field with the magnetization on either side of the ith grain boundary, and L is a mean grain diameter.

The magnetic-pole energy per unit area of surface after domain creation can be shown to be[9]

$$\sigma_i = \frac{1}{3} \pi \omega^{*2} L \left\{ (2\pi r^2/D^2)-1 \right\}^2 + \text{(harmonic terms)}.$$

There are many mechanisms which contribute to the critical field for irreversible domain-wall motion. One mechanism is the contribution $H_{wi}(\omega^{*})$ due to the work required to overcome the grain-boundary-pole energy if the walls are expanded beyond the point $r = D/(2\pi)^{1/2}$. The equilibrium relation $D^2 \Delta \sigma_i = 2 H_{wi}(\omega^{*}) \cdot I_s \Delta V$ gives

$$H_{wi}(\omega^{*}) \approx \frac{\pi \omega^{*2}}{3 I_s} \left\{ (2\pi r_c^2/D^2) - 1 \right\} , \tag{4}$$

where the contribution from the harmonic terms is neglected, and r_c is the critical radius for irreversible wall motion. If these surfaces were lamellar precipitates or if precipitation occurs at the grain boundary, ω^{*} and H_{wi} would be large, $H_{ni} < 0$. An increase in ω^{*} due to inhomogeneities from grain to grain will also decrease H_{ni} and increase $H_{wi}(\omega^{*})$

to possibly destroy loop squareness. Conversely, a decrease in ω^* due to a decrease in $\langle (\cos \Theta_1 - \cos \Theta_2)^2 \rangle$ under an applied stress can increase H_{ni}, decrease $H_{wi}(\omega^*)$.

If the reverse domains are prolate ellipsoids, there is a surface tension in the walls which resists domain growth. Since $\lambda = r/\ell \ll 1$, the surface-tension contribution to the critical field for irreversible wall motion is

$$ H_w(\sigma_w) \approx \sigma_w / (2 I_s r_c \cos \Theta), \text{ where } \underline{H} \cdot \underline{I}_s = H I_s \cos \Theta, \tag{5} $$

There is also the contribution $H_w(\text{incl})$ which is due to the interaction of granular inclusions with the domain walls. The inclusions may be classified into two types: those at which closure domains form and those at which they do not. If a domain-free inclusion is embedded in a wall, the energy of that wall is decreased first by the decrease in domain-wall area, second by the reduction of demagnetizing fields associated with the free ples at the inclusion surface. Therefore there is a tendency for the walls to stick at the inclusions. If the inclusions are randomly distributed through the material, any wall will, on the average, intersect the same number of inclusions: therefore the effect on the coercivity is smaller than originally estimated by Kersten[13]. Néel[14] and Dijkstra[15] have developed independent expressions using different averaging techniques. Experimentally[15] it is observed that this contribution to the coercivity increases with particle size until the mean particle size is approximately δ, the width of a 180° domain wall.

When a mobile wall passes through an inclusion with an associated closure domain, the closure domain remains terminated in the mobile wall[16]. As the wall moves away from the inclusion, the closure domain

is elongated before it snaps free. The surface tension of the closure domains provides a force to keep the mobile wall at the inclusion. This interaction may be written as[10]

$$H_w(\text{incl}) \propto P^{2/3}\sigma_w/(I_s\langle R\rangle) \text{ for } R \gg \delta, \tag{6}$$

where P is the percentage of granular inclusion in the matrix with average granular radius $\langle R\rangle$. This expression can only be valid for $R > \delta$ since only then can the inclusion support a closure domain. This contribution drops off with increasing particle size. Experimentally[15] the maximum coercivity occurs at $\langle R\rangle \approx \delta$.

There are other lattice imperfections which also contribute to the coercive force such as local magnetic-pole densities about dislocations or chemical inhomogeneities and local lattice strains about inclusions and dislocations.[17,18] Since these and $H_w(\text{incl})$ are independent of r_c while $H_w(\omega^*) < 0$ if $r < D/(2\pi)^{1/2}$, the critical radius for irreversible wall motion will lie in the range $D/(2\pi)^{1/2} < r_c < D/2$, and $H_w(\omega^*) \leq \pi\omega^{*2}/(6I_s)$.

In conclusion, a prerequisite for a low-coercivity ferrite is a dense, homogeneous, single-phase, annealed material. Then the coercivity is given by

$$H_c \lesssim a_1\sigma_w/(2I_sL) + \frac{\pi}{6}I_s\langle(\cos\theta_1 - \cos\theta_2)^2\rangle, \tag{7}$$

where a_1 is a factor of order 10 representing the fraction $L/\langle r_c\cos\theta\rangle$. In ferrites the spontaneous magnetization is generally sufficiently small that the first term of Eq. (7) predominates. Therefore after the elimination of inhomogeneity and inclusions (porosity or second phase), the first-order control on coercivity in ferrites is obtained by a proper selection of composition to determine an appropriate value for $\sigma_w/I_s \propto (K'T_c)^{1/2}/I_s$.

A second-order control is then possible by proper processing procedures: bodies are fired for a sufficient length of time and in appropriate atmospheres to establish a homogeneous single phase with equilibrium density and mean grain size L corresponding to a carefully selected and controlled temperature. Fig. 3 illustrates the time of sinter and degree of temperature control required for the ferrite memory cores used in a 256 x 256-bit array. Yields of over 90 per cent cores with satisfactory uniformity were obtained from preparation to preparation (90,000 cores per furnace load).

Also, if a high retentivity is desired, it is necessary to have $H_n' > 0$, where H_n' is the critical field strength for the creation of reverse domains in addition to those already present at $H = H_m$. From Eq. (4) it is apparent that this can be controlled by making

$$A_2 \sigma_w / L > \omega^{*2} = I_s^2 \langle (\cos \Theta_1 - \cos_2)^2 \rangle . \tag{8}$$

In metals with a given σ_w and I_s, this is commonly accomplished by reducing $(\cos \Theta_1 - \cos \Theta_2)$ by rolling to give grain orientation or by provision of a grain-orientation-independent axis of easy magnetization by application of a tensile stress or a magnetic anneal.* Similar treatments are used to obtain metals with square B-H loops. In ferrites with negative magnetostrictive constants the B-H loop can be squared by the application of a compressive stress,[19] see Fig. 4. A more practical method of obtaining square-loop ferrites, however, has been to use ferrites with sufficiently small I_s, large $\sigma_w \propto (T_c K')^{1/2}$ to satisfy Eq. (9) even though there is little to no grain-to-grain alignment of the spontaneous magnetization. A large value of K' also reduces rotational contributions. Finally, a maximum in the squareness ratio has been correlated with zero $\langle 111 \rangle$ magnetostriction;[20,21] this appears to be a second-order effect

---

* For a discussion of illustrative experiments, see ref (10).

and may be interpreted as the result of a partial reduction in

$\langle (\cos \Theta_1 - \cos \Theta_2) \rangle$.

Before leaving the topic of loop shape, it is important to note

that a combination of Eqs. (3) and (7) with $A_2 \approx 30$ and $a_1 \approx 10$ gives the

following limitation for square-loop materials:

$$(B_s/H_c') < 20/\langle (\cos \Theta_1 - \cos \Theta_2)^2 \rangle \; ; \; H_c' = H_w(\omega^*) + H_w(\sigma_w). \tag{10}$$

Unless grain-to-grain alignment of the magnetization can be achieved, this

limitation is serious for applications requiring square-loop ferrites of

large flux density and low coercivity.

(2.3) Permeability:

The permeabilities of interest in magnetic-core circuits are

usually the d.c. incremental permeabilities at remanence, $\mu_{\Delta\pm} = (\Delta B/\pm \Delta H)_{B_r,0,}$

and the initial permeability $\mu_o = (\Delta B/\Delta H)_{B=H=0}$. From Eq. (2) it

follows that

$$(\mu_j - 1)/4\pi = -\frac{I_s}{\Delta H} \left\{ (1 - v_j' - 2v_j) \langle \sin \Theta\Delta\Theta \rangle_1 + v_j' \langle \sin \Theta\Delta\Theta \rangle_2 \right.$$

$$\left. + 2v_j \langle \sin \Theta\Delta\Theta \rangle_3 + \langle \cos \Theta \rangle \Delta(v' + 2v) \right\} \tag{11}$$

where μ_j is either μ_Δ or μ_o, $\langle \sin \Theta\Delta\Theta \rangle_i$ are averages over different

ranges of angle. The terms involving $\Delta\Theta$ are the contributions due to

pure rotation, those involving $\Delta(v' + 2v)$ are due to domain-wall motion

and domain creation in the interval ΔH.

The change in energy of a ferrite subject to a small ΔH causing

a small $\Delta\Theta$ is

$$\Delta E \approx |K'| (\Delta\Theta)^2 - (\Delta H)I_s \cos(\Theta + \Delta\Theta).$$

In a cubic crystal with only crystalline anisotropy, the first order anisotropy energy is $E_k = K_1(\alpha_1^2 \alpha_2^2 + \alpha_2^2 \alpha_3^2 + \alpha_3^2 \alpha_1^2)$, where the α_i are direction cosines for the saturation magnetization. In most ferrites the easy magnetization axis is a $\langle 111 \rangle$ so that $K_1 < 0$ and the $\alpha_i = 1/\sqrt{3}$. It can be shown that in these crystals the effective anisotropy constant $|K'|$ should be replaced by $2|K_1|/3$ in the expression for ΔE. Optimizing with respect to $\Delta\Theta$ gives $\Delta\Theta = -\alpha \sin\Theta/(1 + \alpha \cos\Theta)$, where $\alpha = (3I_s\Delta H/4|K_1|)$. Therefore in a cubic ferrite with $K_1 < 0$, the contribution to the initial permeability from domain rotation is, from Eq. (11),

$$\frac{(\mu_{or}-1)}{4\pi} = \frac{I_s^2}{|K_1|}\left\{ 0.27 + 0.4\ v_o' + 0.15\ (4v_o - 1)\ \frac{I_s(\Delta H)}{|K_1|} \right\}. \quad (12)$$

Previous workers[11,22] have assumed a completely random distribution of magnetization directions in which $v_o' = 1/\sqrt{3}$ and have neglected the second-order terms in α. With these assumptions the domain-rotation contribution to the initial permeability is

$$(\mu_{or} - 1) = 2\pi I_s^2/|K_1|. \quad (13)$$

If in the demagnetized state the domain walls are predominantly 180° walls, few closure domains exist, and the assumption that $v_o' = 1/\sqrt{3}$ is not valid. Further, it is extremely dangerous to assume that the domain-wall contribution to the coercivity is negligible if domain walls exist in the material.

Without a knowledge of the density of domain walls and their distribution, it is impossible to calculate quantitatively the domain-wall contribution to the initial permeability. However, it is possible to postulate a domain-wall density and configuration at the remanence point of a high-retentivity material $(B_r > B_s/2)$. With a model in which the mobile walls are those surrounding cylindrical reverse domains

created at grain boundaries, Eq. (11) becomes

$$(\mu_\Delta - 1)/4\pi \approx (\mu_{\Delta r} - 1)/4\pi + 6v_\Delta \left\{ \langle \Delta r \cos\theta/r_o \rangle + \langle (\Delta r/r_o)^2 \cos\theta \rangle \right.$$

$$\left. + \langle \Delta n(\cos\theta)/n \rangle \right\} I_s/(\Delta H), \qquad (14)$$

where $\Delta n/n$ is the relative change in the number of reverse domains in the interval ΔH. Cylindrical domains in place of ellipsoidal domains of large eccentricity simplify the mathematics without introducing any significant error. The equilibrium value of r is found by minimizing with respect to r the energy per unit length

$$E_\lambda = -2(\Delta H_{eff}) \cdot I_s \pi r^2 + \sigma_w 2\pi r + \frac{\sigma_o}{\lambda} D^2 \left(\frac{2\pi r^2}{D^2} - 1 \right)^2$$

associated with a reverse domain. If $H_1 = H_w(\text{incl.}) + H_w(\text{disl.})$, then $\Delta H_{eff} = (\Delta H - H_1)$ is the effective driving field on the domain wall. Since $\sigma_o/\lambda \approx \omega^{*2}$ and the equilibrium value of r for $\Delta H = 0$ is $r_o = (D/(2\pi)^{1/2}) - \delta r$, where $(\delta r(2\pi)^{1/2}/D) \ll 1$, it follows that $r_o \approx (qL/8) \left[1 - \sigma_w/(qL\omega^{*2}) \right]$ if it is assumed that $qL \approx 8D/(2\pi)^{1/2}$. Thus for small, reversible Δr it follows that

$$\left\langle \frac{\Delta r \cos\theta}{r_o} \right\rangle \approx \beta \left\langle \frac{\cos^2\theta}{1 - \beta \cos\theta} \right\rangle, \text{ where } \beta = \frac{1}{4} \left(\frac{I_s \Delta H_{eff}}{\langle \omega^{*2} - 3 \sigma_w/qL \rangle} \right).$$

The dimensionless parameter q is of order unity for L equal to a mean grain diameter. Since $\Delta n \approx 0$ for small ΔH, substitution into Eq. (14) gives

$$\frac{\mu_\Delta - 1}{4\pi} = \frac{I_s}{\Delta H} \left\{ 0.36\alpha \left(1 + 1.47 \, v_\Delta' + (3v_\Delta - .75)\alpha \right) + 4.4 \, v_\Delta \beta (1 + 15\beta) \right\},$$

$$(15)$$

where higher powers in β are neglected. The second term vanishes if $H_1 > \Delta H$. The volume v_Δ may be estimated as $(v_\Delta + v_\Delta'/2) = (B_s - B_r)/(2 B_s)$.

In dense, single-phase ferrites $v'_\Delta \approx 0$, $H_1 \approx 0$ and to first powers in α, β

$$\frac{\mu_\Delta - 1}{4\pi} \approx 0.27 \frac{I_s^2}{|K_1|} \left\{ 1 + 2(1 - \frac{B_r}{B_s}) \frac{|K_1|}{\langle \omega^{*2} - 3\sigma_w/L \rangle} \right\}. \qquad (15')$$

Experimental values for μ_Δ with $\Delta H = 1$ oe. in magnesium-manganese memory-core ferrites[*,23] are $\mu_\Delta = 50-500$. From Eq. (15') the estimated contributions from domain rotation and domain-wall motion are, respectively, ~ 1 and ~ 200.

Of particular interest to the noise problem in a magnetic-memory matrix is the difference $\Delta_\mu = \mu_{\Delta+} - \mu_{\Delta-}$, where the incremental permeabilities $\mu_{\Delta+}$, $\mu_{\Delta-}$ are those, respectively, for positive and negative ΔH. (Positive ΔH is in the demagnetizing direction). From Eq. (15) it follows that

$$\Delta_\mu = 3.8 \frac{I_s^3 (\Delta H)}{K_1^2} \left\{ (1 - \frac{B_r}{B_s}) \left[2 + 7 \left(\frac{K_1}{\omega^{*2} - 3\sigma_w/L} \right)^2 \right] - 1 \right\}. \qquad (16)$$

For $\Delta H = 1$, the estimated values of Δ_μ for a magnesium-manganese memory core are $\Delta_\mu \sim 40$. The corresponding experimental values[23] were $\Delta_\mu = 10-100$.

Finally it should be pointed out that the amplitude permeability $\mu \cong B_m/H_m$ decreases with increasing frequency[11]; at higher frequency the applied field is in the neighborhood of its maximum value for shorter times, and smaller irreversible wall motions result. This effect is more pronounced the larger the fraction of the permeability resulting from wall motion.

(2.4) Flux Reversal

In many circuits magnetic cores are driven by square-wave current pulses. In these circuits the shape, peak voltage, and duration

---

* The assumption in ref (23) of $E = pr^2$ instead of $p[(2\pi r^2/D^2)-1]^2$ cannot be justified as $(2\pi r^2/D^2)$ is not very different from 1 in the range $0 \leq H \leq \Delta H$.

of the output pulse on the secondary are of interest. The principal
mechanism for flux reversal is the creation and/or growth of domains of
reverse magnetization by the motion of the 180° domain walls which
surround them. According to the model of this paper, these reverse do-
mains are ellipsoids of such large eccentricity that they may be well
approximated by cylinders. The retarding forces per unit area of the
wall can be expressed as energy per unit volume $2\underline{H}_o \cdot \underline{I}_s$, where H_o is the
threshold field for which the average velocity of the walls vanishes.
Since the mass per unit area of wall is small, $m \sim 10^{-10}$ gm/cm^2, in first
approximation the equation of motion of the walls of the expanding domains
is[24]

$$\beta \frac{d\langle r\rangle}{dt} = 2I_s(H_m - H_o) \langle \cos \Theta\rangle^2, \tag{17}$$

where β is a viscous-damping parameter and Θ is the angle between the
applied field $\underline{H}_m$ and the magnetization $\underline{I}_s$ in a particular grain. Eq. (17)
assumes an ideally square input pulse. Therefore it is valid only when
the rise time t_r of the input pulse is small compared to the switching
time τ. Also because H_o represents an average over all the walls which
move, it has a constant value only for driving fields greater than the
critical field H_w(max) required to move all the mobile domain walls.
However, it is a good approximation within the limits H_w(max)$<H_m<H(t_r/\tau<0.3)$.

The viscous-damping parameter $\beta = \beta_e + \beta_r$ is composed of an eddy-
current and a relaxation contribution. For practical interest ferrites
must have a sufficiently large resistivity that $\beta_e/\beta_r \ll 1$. The eddy-
current contribution is therefore neglected. The mechanisms responsible
for relaxation damping are not known. It has recently been suggested[25]
that they are due to relaxation losses in the elastic constants, these
losses being measurable as ferromagnetic losses because of magnetoelastic

coupling. Although the precise origin of this damping is not yet known, its effect can be reasonably expressed by a phenomenological equation of angular motion first proposed by Landau and Lifshitz:[26]

$$\frac{d\underline{I}}{dt} = \gamma(\underline{I} \times \underline{H}) + \Lambda (\underline{I} \times \underline{H} \times \underline{I})/I^2,$$

where $\gamma = ge/2mc$ is the magneto-mechanical ratio and Λ is an intrinsic relaxation frequency. From this equation it can be shown[24] that

$$\beta_r = 2 \Lambda (K'/\Lambda)^{1/2}/\gamma^{*2}; \quad \gamma^{*2} = \gamma^2 + \Lambda^2/I_s^2.$$

Since β_r is independent of $\langle r \rangle$, integration of Eq. (17) gives

$$(H_m - H_o)\tau = S_w \approx \frac{\Lambda d}{I_s \gamma^{*2}} \left(\frac{K'}{\Lambda}\right)^{1/2} \approx \frac{7\Lambda}{I_s \gamma^{*2}} \left(\frac{d}{\delta}\right), \tag{18}$$

where d is the distance a wall moving with average velocity $d \langle r \rangle /dt$ travels during the flux-reversal time τ, and S_w is defined as the switch-ing coefficient.[*] In the application of Eq. (18), it must be appreciated that d and H_o may be considered independent of H only in square-loop materials. In a coincident-current memory the driving fields are re-stricted to $(H_m - H_o) \approx H_c$. For a low-power, high-speed memory it is necessary to have a small S_w. Present square-loop ferrites have $S_w \approx 1 + 0.5$ oe-μsec. If a core should switch by domain rotation rather than wall motion, then $d/\delta = 1$ and the numerical coefficient is halved since the switching can be described by the motion of a plane wall moving one wall width δ: in such a material S_w would be reduced by a factor of nearly 100.

The shape of the output voltage on the sense winding is a measure of the rate of change of flux through the magnetic core:

[*] For typical plots of H_m vs. $1/\tau$, see refs.(24),(36) where the properties of square-loop ferrites are compared with those of metallic ribbon cores.

$$\frac{d\Phi}{dt} = 2 \langle\cos\Theta\rangle B_s \sum_i \frac{dA_i}{dt} = \frac{16\pi I_s^2 \langle\cos\Theta\rangle^3}{\beta} (H_m - H_o) \sum_i \frac{\partial A_i}{\partial\langle r\rangle},$$

(19)

where A_i is the area of intersection of the ith reverse domain with some

cross-sectional area of the core. Since the domain walls are accelerated

to their average velocity within the driving-pulse rise time of 0.2 μsec,

the shape of the output voltage for a given H_m is determined by

$\sum_i \partial A_i/\partial\langle r\rangle$. Both reversible and irreversible domain creation and/or

growth contribute to the flux change. With a model of cylindrical reverse

domains, $\partial A_i/\partial\langle r\rangle > 0$ for values of r which are too small for collision

of reverse domains. The reversible motions contribute an output voltage

which rises to a maximum at the end of the pulse rise time and then falls

off sharply, the walls reaching their equilibrium position for H_m at the

end of the rise time. After t_r, however, the output voltage due to

irreversible domain growth continues to increase with increasing domain-

wall area until the various reverse domains collide with one another:

subsequently the output voltage decreases as the colliding domain walls

annihilate each other. Since $\langle r\rangle$ is a function of time through Eq. (17),

the irreversible domain growth produces an output voltage which is a

unimodel function of time. Its maximum shifts to shorter times with in-

creasing H_m. Because of a random distribution of reverse domains, at

larger r, or longer time, the term $\sum_i \partial A_i/\partial\langle r\rangle$ falls to zero with a

Gaussian-like tail. A typical output voltage from a magnesium-manganese

memory core driven by different fields H_m is shown in Fig. 5. The first

small peak due to irreversible effects is nearly swamped by the large

peak if H_m is large.

Finally since in any given core $\sum_i \partial A_i / \partial \langle r \rangle$ may reasonably be assumed to vary with $\langle r \rangle$ independently of the wall velocity for $H_w(\max) < H_m \langle H(t_r/\tau < 0.3)$, the peak voltage $_uV_1$ is seen from Eq. (19) to vary directly with the driving field:

$$(H_m - H_o) = S_v \left(_uV_1 \right) \qquad (20)$$

where $S_v \propto \beta/I_s^2$ is a constant of the material. In contrast to S_w, the coefficient S_v is independent of the loop squareness; it is therefore the more useful parameter for materials with nonsquare loops. It can be shown[35] that corrections to S_w for a nonsquare-loop material can be made from a knowledge of S_v. In Fig. 6 the loop shape and switching coefficients of a Ferroxcube-103 core are plotted as a function of an externally applied compressive stress. Presumably the smaller number of reverse domains participating in the switching causes R_s and $S_v, S_w \propto d$ to increase with stress while the increase in K' influences $H_o \propto \sqrt{K''}$.

(2.5) Temperature Limitations

For a square-loop ferrite the total energy loss W per unit volume per cycle is, under the approximations inherent in Eq. (17),

$$W \approx 2H_o I_s \langle \cos \theta \rangle + \beta_r d/\tau + \text{(eddy-current losses)}.$$

In some high-permeability materials Wijn[11] has shown that beside the usual losses associated with β_r, there are residual losses at low frequencies which are due to a relaxation phenomenon resulting from the diffusion of electrons. These residual losses are most pronounced when ferrous and ferric ions are both present on the octahedral sites. To minimize this effect, ferrites should be prepared so as to minimize the number of ferrous ions present. This also makes the eddy-current losses negligible.

The energy W is dissipated as heat within the core. Since ferrites are poor thermal conductors, this heat is not readily removed from the core. Therefore if the core is switched at a high repetition rate, it will be operating at a temperature which is considerably above the ambient temperature. Since the characteristics of the material degenerate rapidly as the Curie temperature is approached, there is an upper repetition-rate limit for a ferrite-core circuit. This limit is optimized by maximizing the Curie temperature and minimizing the core dimensions. The temperature limitations for a magnesium-manganese ferrite operated as an information-storage device are indicated in Fig. 8.

(3) Microscopic Considerations

In first approximation the theory of ferrites assumes that these materials are ionic. From this model it is possible to estimate the electrostatic binding energy, the elastic moduli, and, on the basis of a packing of hard spheres, the lattice parameters and gross crystal structure (rock salt, spinel, perovskite, etc.). From this model it has also been possible to explain the very large variations in electrical resistivity ρ. Verwey[27] has demonstrated that if two cations of the same atom but different ionization are randomly present on the same type of lattice site, the resistivity is reduced. This is important for the ferrites where Fe^{2+} and Fe^{3+} are often both present on the octahedral sites. However, this approximation gives incomplete information about cation affinities for tetrahedral vs. octahedral interstices in a close-packed anion lattice and can give no information about certain lattice distortions from close-packed symmetry, the indirect magnetic-exchange interactions by which the cation magnetic moments are coupled via an

intermediary anion, and crystalline or magnetostrictive anisotropy. To understand these properties which, in the ferrites, determine the important parameters I_s, T_c or A, and K', it is necessary to have a second approximation. If this approximation is to be useful for the materials manufacturer, it must be easily visualized qualitatively and correlate observed data; it should also suggest the essential features for a quantitative calculation.

Such a second approximation has been proposed.[26] It is cast in the language of directed orbitals and covalent bonding[29] to make its qualitative features more readily visualized. It assumes that the 3d, 4s, and 4p atomic orbitals, which are of nearly the same energy, may become hybrid orbitals in the crystal lattice. If there are low-energy cation orbitals which are empty and strongly overlap full anion orbitals, the cation-anion bond will be partially covalent, the anion sharing its outer electrons with the cation. The degree of covalence is given by $a^2/\Delta E$, where a varies with the orbital overlap and ΔE is the energy difference between the ionic and excited (covalent) state of the system. The number of electrons in a cation d shell determine the possible low-energy, hybrid orbitals which are completely empty, and the lattice symmetry about the cation determines whether these empty orbitals can strongly overlap the full anion orbitals. The factors which determine the cation affinity for a given anion interstice are the electrostatic energy, the cation size, and the degree of covalence or sharing of anion electrons with neighboring cations via the overlapping orbitals. What determines the cation distribution in a particular spinel lattice is the relative affinities the cations of that spinel have for the tetrahedral or octahedral interstices.

In Table I are indicated the angular dependencies of the
possible atomic orbitals of interest together with their azimuthal quan-
tum number m indicating the component of the orbital angular momentum on
the axis $\Theta = 0$. The effect of the crystalline, cubic electric fields is
to split the atomic d energy level into two energy levels. The level d_e
is doubly degenerate containing the orbitals (expressed in terms of their
angular dependence only) $d_{xy} = \sin^2\Theta \cos \phi$, $d_z = (3 \cos^2\Theta - 1)$; the level
d_t is triply degenerate containing $d_{x+y} = \sin^2\Theta \sin \phi$, $(d_{x+z} \pm d_{y+z}) =$
$\sin \Theta \cos \Theta \, e^{\pm i\phi}$. The orbitals d_e are directed along the three cubic axes.
Where the spatial directions are specified, the angular momentum is not
known in accordance with the Uncertainty Principle. Therefore the split-
ting of the energy level makes $m = 0$ for d_{xy} and d_{x+y}. This is referred
to as "quenching" of the orbital angular momentum. Further, if a cation
is in an octahedral site, the energy level $d_e > d_t$ to provide, if possible,
an empty orbital extending toward the neighboring anions. Conversely if
a cation is in a tetrahedral site, $d_t > d_e$. Since this splitting may be
assumed weaker than the splitting due to the atomic exchange interactions,
the atomic d energy levels within octahedral (or B) and tetrahedral (or A)
interstices of a close-packed-cubic anion lattice may be schematically
represented as in Fig. 8. Finally the significant hybrid orbitals are
tetrahedral (sp^3), tetrahedral (d^3s) using d_t, octahedral (d^2sp^3) using
d_e, and square (dsp^2) using d_{xy}. From these considerations it is
possible to construct Table II. It must be emphasized that the degree
of covalence for cations of similar outer-electron configuration will
vary from ion to ion so that the column "covalent interstice affinity"
must be recognized as offering, at best, a qualitative rule of thumb.
Besides, relative cation charges and sizes must also be considered before

TABLE I: <u>Angular Dependence</u> and <u>Azimuthal</u> Quantum <u>Numbers</u> of <u>Atomic</u> Orbitals

<u>Atomic Orbital</u>	<u>Angular</u> Dependence	$\underline{m}$
s	1	0
p	$\sin\theta\, e^{\pm i\phi}$	± 1
	$\cos\theta$	0
d	$\sin^2\theta\, e^{\pm 2i\phi}$	± 2
	$\sin\theta\cos\theta\, e^{\pm i\phi}$	± 1
	$(3\cos^2\theta - 1)$	0

TABLE III: Order of cation stability in A sites of oxygen spinels: (Estimated on basis of available experimental data)

MOST STABLE		In^{3+}		Li^+, V^{3+}
Zn^{2+}, Ge^{4+}		Mg^{2+}, Cu^{2+}		Mn^{3+}, Sn^{4+}
Cd^{2+}		Ti^{4+}		Cr^{3+}
Mn^{2+}		Co^{2+}, Fe^{2+}		Mn^{4+}, Ni^{2+}
Ga^{3+}, Fe^{3+}		Al^{3+}		LEAST STABLE

TABLE II: CATION CHARACTERISTICS DEDUCED FROM HYBRID-ORBITAL HYPOTHESIS

(d_t and d_e are triply and doubly degenerate energy levels of d orbitals split by cubic crystalline field; m is azimuthal angular-momentum quantum number)

Elec. Config.	Cations	Ion Site	Number of electrons in d_t	Number of electrons in d_e	Covalent Orbitals†	Exchange Orbitals Υ	Covalent Interstice Affinity	m along a ⟨100⟩	Speculated Contrib. to λ_{111}	Interstice Distortion	Magnetic Moment in Bohr Magnetons Ferri-	Magnetic Moment in Bohr Magnetons Para-
d^2	$V^{3+}Cr^{4+}$ $Mo^{4+}Ru^{6+}$ $W^{4+}Os^{6+}$	A	0	half full	None	(d^3s)	+	0	< 0	None	2	2.83
		B	2	0	None	(d^2sp^3)	+	1	> 0			
d^3	$V^{2+}Cr^{3+}Mn^{4+}$ Mo^{3+}	A	1	half full	None	$\{(d^3s)\}$		1	> 0	None	3	3.88
		B	half full	0	None	(d^2sp^3)	++	0	< 0			
d^4	$Cr^{2+}Mn^{3+}Fe^{4+}$ $Mo^{2+}Ru^{4+}$ Os^{4+}	A	2	half full	None	$\{(d^3s)\} + (sp^3)$	0	1	> 0	None	4	4.90
		A	half full	1	$(dsp^2)*$	$(dsp^2)*$	+	?	> 0	c/a < 1		
		B	half full	1	(dsp^2)	$(dsp^2) + [d_z]†$	+++	?	> 0	c/a > 1		
d^5	$Mn^{2+}Fe^{3+}Co^{4+}$ Ru^{3+} $Os^{3+}Ir^{4+}$	A	half full	half full	(sp^3)	$\{(d^3s)\} + (sp^3)$	+++			None	5	5.91
		B	half full	half full	None	$\{(d^2sp^3)\}$	+	0	< 0			
d^6	$Fe^{2+}Co^{3+}$ $Ru^{2+}Rh^{3+}Pd^{4+}$ $Ir^{3+}Pt^{4+}$	A	half full	half + 1	None	(sp^3)	+	0	< 0	None	4	4.90
		B	half + 1	half full	None	$\{(d^2sp^3)\}$	+	1	> 0			
d^7	$Co^{2+}Ni^{3+}$ Rh^{2+}	A	half full	full	None	(sp^3)	+	0	< 0	None	3	3.88
		B	half + 2	half full	None	$\{(d^2sp^3)\}$	+	1	> 0			
		B	full	1	(dsp^2)	$(dsp^2) + [d_z]†$	+++	0	< 0	c/a > 1	1	1.73
d^8	Ni^{2+} $Rh^+Pd^{2+}Ag^{3+}$ $Pt^{2+}Au^{3+}$	A	half + 1	full	None	(sp^3)	0	1	> 0	None	2	2.83
		B	full	half full	None	$\{(d^2sp^3)\} + \{(dsp^2)\}$	++	0	< 0			
		B		d_e^2	(dsp^2)	--	+++	-?	--	c/a > 1	0	0
d^9	Cu^{2+}	A	half + 2	full	None	(sp^3)	++	1	> 0	None	1	1.73
		A	full	$d_e^2 + [1p]$	$(dsp^2)*$	$(dsp^2)*$	++	?	> 0	c/a < 1		
		B	full	$d_e^2 + [1p]$	(dsp^2)	(dsp^2)	+++	?	> 0	c/a > 1		
d^{10}	$Zn^{2+}Ga^{3+}Ge^{4+}$ $Cd^{2+}In^{3+}Sn^{4+}$	A	full	full	(sp^3)	--	++++	0	--	None	0	0
		B	full	full	None	--	0	0	--			
		B	full	$d_e^2 + [2p]$	(dsp^2)	--	++	0	--	c/a > 1		

* Lattice distortion increases partial orbital overlap and shifts level d_e relative to level d_t.

† Empty (dsp^2) overlaps 4 coplanar neighbors; half-filled d_z overlaps other two neighbors.

† Empty, low-energy orbitals with large anion overlap.

Υ Orbitals available for semicovalent exchange. $\{\}$ if partially filled.

an estimate of probable cation distribution can be made. If no obvious assignment of interstice location is possible, the entropy is an important factor distributing the cations randomly over the two types of sites. In Table III the cations commonly found in spinel-type lattices are listed in order of their experimental stability in A sites.

To calculate I_s at $0^{\circ}K$, it is only necessary to assume* that the ions on the A sites have their moments aligned parallel to one another and antiparallel to those on the B sites. This type of magnetic coupling holds generally in the ferrites unless the major percentage of A-site ions are nonmagnetic as in Zn^{2+}-substituted materials. An appropriate correction[30] must be made in the case $g \neq 2$.

In ferrites of practical interest, the Curie temperature T_c or the exchange constant A are primarily determined by the strength of the A-B coupling, the coupling of the A-site magnetic moment with the B-site moment. This coupling is indirect, an anion playing the role of an intermediary. In a cubic lattice the anion p orbitals, if they are not hybridized with the s orbital through covalent bonding with tetrahedrally located neighbors, have (see Table I) the angular dependence $p_x = \sin \Theta \cos \phi$, $p_y = \sin \Theta \sin \phi$, $p_z = \cos \Theta$ and are directed as in Fig. 9(a). By the Pauli Exclusion Principle each full orbital contains a pair of antiparallel electrons. If the anion overlaps an empty cation orbital of low energy (represented schematically in Fig. 9 by a straight line from the cation), the anion-cation bond is partially covalent. Further if the cation possesses a directed magnetic moment, the anion electron whose moment is parallel to that on the cation will be the more stable in the covalent bond (extension of Hund's rule). If another cation is similarly

* For the theory of $I_s(T)$ in ferrites refer to refs. (1),(2),(5).

situated on the opposite side of the anion, the lowest energy state is
that in which each of the two anion electrons has the opportunity to be
the dominant electron in a covalent (or semicovalent since one electron
predominates) bond. This gives rise to antiferromagnetic coupling such
as occurs between the A- and B-site cations of the usual ferrite. If
the second cation happens to be one with low-energy orbitals designated
$(dsp^2) + [1d_z]$ in Table II which are oriented as shown in Fig. 9(b), then
the second anion electron is oriented antiparallel to the net moment of
that cation because of the Exclusion Principle, and the two cations are
ferromagnetically coupled.[*] Because of the indirect nature of the mag-
netic coupling, the magnitude of T_c or A varies with the degree of
covalent bonding as well as with the magnitude of the cation magnetic
moments and the percentage of A and B sites which are occupied with mag-
netic ions. Variations in the Curie temperature of a ferrite with
additions of nonmagnetic Zn^{2+} in A sites in place of nonmagnetic Mg^{2+} in
B sites is illustrated in Fig. 10. With added Zn^{2+} there is also an
initial increase in B_s with a corresponding decrease in H_c.

Whenever empty, low-energy (dsp^2) orbitals are available for
covalent bonding, there is a possibility of lattice distortions. These
orbitals point toward the four corners of a square. If they exist in B
sites, four coplanar bonds are more stable than the two ionic bonds
perpendicular to this plane, and the site is distorted to tetragonal
symmetry with c/a > 1. If enough of these distorted sites exist, below
a critical temperature they order to reduce the elastic energy of the
lattice, and the entire crystal becomes tetragonal[§] (c/a > 1). If these

---

[*] For an illustration of this type of coupling, see refs.(31),(32).
[§] For a further discussion see ref. (28).

TABLE IV: Some tetragonal spinels

Composition	Axial Ratio c/a
Mn_3O_4	1.16[a]
γMn_2O_3	1.16[b]
$ZnMn_2O_4$	1.16[c]
$CoMn_2O_4$	1.14[a]
$CuCr_2O_4$	0.914[a]
$CuFe_2O_4$	1.06[d] *
$NiCr_2O_4$	1.025[e]
$CdIn_2O_4$	1.14[f] §
$CaIn_2O_4$	1.12[f]

* Varies with heat treatment, or number of Cu^{2+} ions in B sites.

§ A Stoichiometric sample $CdIn_2O_4$ prepared at Lincoln Laboratories by D. Wickham and W. Croft was cubic (a = 9.16 Å).

a. D. Wickham and W. Croft, unpublished research
b. E. J. W. Verwey and J. H. de Boer, Rec. trav. chim 55, 531 (1936)
c. B. Mason, Am. Minerologist 32, 426 (1947)
d. E. F. Bertaut, J. phys. radium 12, 252 (1951)
e. F. K. Lotgering, Thesis, Univ. of Utrecht (Mar. 1956) to appear in Philips Res. Rep.
f. L. Passerini, Gazz. chim. ital. 60, 754 (1930)

orbitals exist in A sites, the A site is distorted by the shift of the four neighboring anions towards a common plane. Steric hindrances prevent the anions from becoming coplanar, but the shift causes a distortion of the lattice* to tetragonal symmetry with $c/a < 1$. Some common tetragonal spinels are listed in Table IV.

Cations with electron configuration d^7 or d^8 cannot form (dsp^2) bonds without a reduction of their magnetic moment: these cations will not form (dsp^2) bonds unless the energy gain due to covalent bonding is greater than the loss in energy due to reversing the electron spin against the exchange forces. From the tetragonal distortion of $NiCr_2O_4$ ($c/a = 1.025$), it appears that the Ni^{2+} ions in the B sites of this spinel do form square bonds.[6,5] The possibility of (dsp^2)-bond formation in the d^{10} cations is small: it requires an energy gain due to covalent bonding in excess of the loss in energy to excite two electrons from a full d shell to a p state. However, there is some evidence[28] (see Table IV) that this can happen in the case of In^{3+}.

The origin of the anisotropy and magnetostriction in ferro-magnetic materials is not yet fully understood. It is generally agreed, however, that if the magnetic ion has an angular momentum which is coupled to the lattice, then the spin-orbit coupling will give rise to a magnetic anisotropy. If, therefore, the azimuthal quantum number m along a $\langle 100 \rangle$ is not zero (see Table II) for a given magnetic cation, its spin-orbit coupling can be assumed to contribute to an easy-magnetization direction along a $\langle 100 \rangle$ axis. Among the few available experiments it is observed that when all the cations of a ferrite are so located that $m = 0$, the

---

* Measurements verifying the nature of the A site distortion in $CuCr_2O_4$ were recently reported by ref.(33).
§ The objection of ref.(5) that the Ni^{2+} are in A sites is not experi-mentally verified and is open to serious question.

easy-magnetization direction is along a $\langle 111 \rangle$ and the $\langle 111 \rangle$ magnetostriction is negative. As a rule of thumb, if it is desired to change the anisotropy from a $\langle 111 \rangle$ direction to a $\langle 100 \rangle$ direction, it is necessary to introduce into appropriate lattice sites cations for which m may be m = 1.

Similarly if it is desired to improve loop squareness or initial permeability by making the $\langle 111 \rangle$ magnetostriction constant vanish (λ_{111} = 0), it may be tentatively assumed that cations so located that m = 0 contribute to $\lambda_{111} < 0$ and cations so located that m $\neq$ 0 contribute to $\lambda_{111} > 0$. It should be noted that Cu^{2+} and d^4-cations such as Mn^{3+} distort their interstice from cubic symmetry. In this instance the cubic symmetry is destroyed and with it the mechanism for orbital-momentum quenching through cubic-field splitting. Additions of these ions have been observed[20,21] to contribute $\lambda_{111} > 0$.

Since m = 1 for Fe^{2+} ions in B sites, any measurements of anisotropy on samples which contain excess iron may be in considerable error when applied to stoichiometric ferrites. The problem is further complicated by the fact that at room temperature the momentum-contributing electron is not localized to the Fe^{2+} ion if Fe^{3+} ions are also present on the B sites. It is only at lower temperatures[34] (T < 130°K) that the easy-magnetization direction of Fe_3O_4 becomes a $\langle 100 \rangle$.

In conclusion, the factors influencing B-H loop shape, coercivity, permeability, flux-reversal time, and energy loss in ferrite cores driven by square-wave pulses have been expressed in terms of structure-sensitive and structure-insensitive parameters. These are summarized in Table V. Further a chemical model has been provided to suggest qualitatively how the structure-insensitive parameters I_s, K_1, λ_{111}, T_c, depend on the chemistry of the spinel lattice. The contributions to the

Design Parameter	Formulae	Factors determining values of basic physical constants
Retentivity	$B_r = 4\pi I_s(1 - v'_\Delta - 2v_\Delta)\langle\cos\theta\rangle$	$I_s, K_1, T_c, \lambda_{111}$: Chemistry
Loop Squareness	$H_n \propto (A_2\sigma_w - L\omega^{*2})$; $A_2 \sim 30$ in ferrites $H_n > 0$ if $(A_2\sigma_w/L) > I_s^2\langle(\cos\theta_1 - \cos\theta_2)^2\rangle$ or $(B_s/H'_c) < 20/\langle(\cos\theta_1 - \cos\theta_2)^2\rangle$ provided dense, homogeneous body without precipitates. $H'_c = H_w(\omega^*) + H_w(\sigma_w)$	$\left.\begin{array}{c}v'_\Delta\\ v'_o\end{array}\right\}$: with porosity v_Δ : inversely with H_n $\left.\begin{array}{c}\langle\cos\theta\rangle\\ \langle(\cos\theta_1 - \cos\theta_2)^2\rangle\end{array}\right\}$: λ_{111} and external stress $\left.\begin{array}{c}L\\ \langle R\rangle\end{array}\right\}$: Processing (time and temp. of sinter, pressing pressure, etc.) P: porosity and precipitates.
Coercivity	$H_c = H_w(\omega^*) + H_w(\sigma_w) + H_w(\text{incl.}) + H_w(\text{lam.ppt.}) + \ldots$ $H_w(\omega^*) \sim \frac{1}{6}\pi I_s\langle(\cos\theta_1 - \cos\theta_2)^2\rangle$ $H_w(\sigma_w) \sim 5\,\sigma_w/(I_s L)$ $H_w(\text{incl.}) \propto P^{2/3}\sigma_w/I_s\langle R\rangle$ for $\langle R\rangle \gg \delta$ (Maximum value occurs for $\langle R\rangle \approx \delta$). $H_w(\text{lam.ppt.}) \sim \sigma_\lambda/(2I_s L_\lambda)$	σ: surface pole density at a lamellar precipitate: varies with thickness of ppt. and I_s. L: mean distance between lamellar precipitates. Λ: (?) H_o: with H_w $\delta \propto (T_c/K')^{1/2}$ d : inversely with L, R_s (Eddy Current): inversely with ρ, with (smallest dim.)^2 $\left.\begin{array}{c}1/\rho\\ (\text{Residual})\end{array}\right\}$: with presence of two cations of same element but different ionization on same sites (Fe^{2+}, Fe^{3+}) $\sum_i \dfrac{\partial A_i}{\partial\langle r\rangle}$: magnetic history and number of active centers for domain nucleation.
Permeability	$(\mu_o - 1) = 2\pi(I_s^2/|K_1|)(0.54 + 0.8\,v'_o) + \text{Wall Contributions}$ $(\mu_\Delta - 1) = 1.1\pi\dfrac{I_s^2}{|K_1|}\left\{1 + 2\left(1 - \dfrac{B_r}{B_s}\right)\dfrac{|K_1|}{\langle\omega^{*2} - 3\sigma_w/L\rangle}\right\}$	
Noise	$\Delta_\mu = 3.8\dfrac{I_s^3(\Delta H)}{K_1^2}\left\{\left(1 - \dfrac{B_r}{B_s}\right)\left[2 + 7\left(\dfrac{K_1}{\omega^{*2} - 3\sigma_w/L}\right)^2\right] - 1\right\}$	
Flux Reversal	$(H_m - H_o)\tau = (\text{Eddy Current}) + \dfrac{3.5}{I_s\gamma^{*2}}\begin{cases}2d/\delta\ (\text{domain walls})\\ 1\ (\text{rotation})\end{cases}$ provided $H_w(\text{Max}) \le H_m \le H(t_r/\tau < 0.3)$	
Output Volt.	$_u V_1 = S_v^{-1}(H_m - H_o)$; $S_v^{-1} \propto \dfrac{I_s^2 d}{\Lambda}\sum_i\dfrac{\partial A_i}{\partial\langle r\rangle}$	
Losses/cycle	$W = 2H_o I_s\langle\cos\theta\rangle + \beta_r d/\tau + (\text{Eddy current}) + (\text{Residual})$	

parameter Λ are not yet understood. Finally the importance of careful control of such structure-sensitive properties as grain size, porosity, precipitates, and material homogeneity have been stressed.

Acknowledgment

References

(1) NÉEL, L.: "Magnetic properties of ferrites; ferrimagnetism and antiferromagnetism," Annales de Physique, 1948, [12] 3, p. 137-198.

(2) YAFFET, Y., and KITTEL, C.: "Antiferromagnetic arrangements in ferrites," Physical Review, July 15, 1952, 87, p. 290-294.

(3) ROMEIJN, F. C.: "Physical and crystallographic properties of some spinels," Philips Research Reports, 1953, 8, p. 304-320.

(4) GORTER, E. W.: "Saturation magnetization and crystal chemistry of ferrimagnetic oxides. I. II. Theory of ferrimagnetism III.," Philips Research Reports, 1954, 9, p. 295-320, p. 321-365.

(5) LOTGERING, F. K.: "On the ferrimagnetism of some sulphides and oxides," Thesis, University of Utrecht, March 1956, (to appear in Philips Research Reports).

(6) MAXWELL, L. R., and PICKART, S. J.: "Magnetization in nickel ferrite-aluminates and nickel ferrite-gallates," Physical Review, December 1, 1953, 92, p. 1120-1126; "Magnetic and crystalline behavior of certain oxide systems with spinel and perovskite structures," Physical Review, December 15, 1954, 96, p. 1501-1505.

(7) CALHOUN, B. A.: "Magnetic and electric properties of magnetite at low temperatures," Physical Review, June 15, 1954, 94, p. 1577-1585.

(8) KITTEL, C.: "Physical theory of ferromagnetic domains," Reviews of Modern Physics, October 1949, 21, p. 541-583.

(9) GOODENOUGH, J. B.: "Interpretation of domain patterns recently found in BiMn and SiFe alloys," Physical Review, April 15, 1956, 102, p. 356-365.

(10) GOODENOUGH, J. B.: "A theory of domain creation and coercive force in polycrystalline ferromagnetics," Physical Review, August 15, 1954, 95, p. 917-932.

(11) SMIT, J., and WIJN, H. P. J.: "Physical properties of ferrites," Advances in Electronics and Electron Physics, 1956, 6, p. 69-136.

(12) GREINER, C.: "Nachweis von Ummagnetisierungskeimen an Eisen-Nickel-Drähten unter Zug mit der Methode der Bitterschen Streifen," Annalen der Physik,15 July 1955, 16, p. 176-180.

(13) KERSTEN, M.: "Grundlagen einer Theorie der Ferromagnetischen Hysterese und Koerzitivkraft," (S. Hirzel, Leipzig, 1943).

(14) NÉEL, L.: "Nouvelle théorie du champ coercitif," Physica, April 1949, 15, p. 225-234.

(15) DIJKSTRA, L. J., and WERT, C.: "Effect of inclusions on coercive
      force of iron," Physical Review, September 15, 1950, 79, p. 979-
      985; KERR, J., and WERT, C., "Effect of nitrides on the coercive
      force of iron," Journal of Applied Physics, September 1955, 26,
      p. 1147-1151.

(16) WILLIAMS, H. J., and SHOCKLEY, W.: "A simple domain structure in
      an iron crystal showing a direct correlation with the magnetiza-
      tion," Physical Review, January 1, 1949, 75, p. 178-183.

(17) VICENA, F.: "On the influence of stresses produced during precipi-
      tation on the coercive force of ferromagnetics," Czechoslovak
      Journal of Physics, February 1955, 5, p. 11-17; "On the influence
      of dislocations on the coercive force of ferromagnetics,"
      Czechoslovak Journal of Physics, 1955, 5, p. 480-488.

(18) BRENNER, R.: "Ergebnisse und Probleme der quantitativen Theorie der
      Koerzitivkraft," Zeitschrift fur angewandte Physik, September 1955,
      7, p. 499-507.

(19) WILLIAMS, H. J., SHERWOOD, R. C., GOERTZ, M., and SCHNETTLER, F. S.:
      "Stressed ferrites having rectangular hysteresis loops,"
      Transactions American Institute of Electrical Engineers (Communi-
      cations and Electronics, November 1953, No. 9, p. 531-537).

(20) WIJN, H. P. J., GORTER, E. W., ESVELDT, C. J., GELDERMANS, P.:
      "Conditions for square hysteresis loops in ferrites," Philips
      Technical Review, August 1954, 16, p. 49-58.

(21) BALTZER, P. K.: "Magnetostriction in ferrites possessing a square
      hysteresis loop," Conference on Magnetism and Magnetic Materials,
      June 14-16, 1955 (Published by American Institute of Electrical
      Engineers, October 1955), p. 247-252.

(22) WEISZ, R. S.: "Initial permeability in ferrimagnetic spinels,"
      Conference on Magnetism and Magnetic Materials, June 14-16, 1955
      (Published by American Institute of Electrical Engineers,
      October 1955), p. 292-298.

(23) CHILDRESS, J. D.: "The noise problem in the coincident-current
      memory matrix," Conference on Magnetism and Magnetic Materials,
      June 14-16, 1955 (Published by American Institute of Electrical
      Engineers, October 1955), p. 210-218.

(24) MENYUK, N. and GOODENOUGH, J. B.: "Magnetic materials for digital-
      computer components. I. A theory of flux reversal in polycrystal-
      line ferromagnetics," Journal of Applied Physics, January 1955,
      26, p. 8-18.

(25) ZEIGER, H. and HELLER, G.: "Magnetoelastic theory of line width,"
      (to be published).

(26) LANDAU, L. and LIFSHITZ, E.: "On the theory of the dispersion of magnetic permeability in ferromagnetic bodies," Physikalische Zeitschrift Sowjetunion, 1935, 8, p. 153-169.

(27) VERWEY, E. J. W. and de BOER, J. H.: "Cation arrangement in a few oxides with crystal structures of the spinel type," Recueil des Travaux Chimiques, 1936, 55, p. 531-540.

(28) GOODENOUGH, J. B. and LOEB, A. L.: "Theory of ionic ordering, crystal distortion, and magnetic exchange due to covalent forces in spinels," Physical Review, April 15, 1955, 98, p. 391-408.

(29) PAULING, L.: "The Nature of the Chemical Bond," (Oxford Univ. Press, London, 1948) second edition.

(30) KITTEL, C.: "On the gyromagnetic ratio and spectroscopic splitting factor of ferromagnetic spinels," Physical Review, September 15, 1949, 76, p. 743-748.

(31) GOODENOUGH, J. B.: "Theory of the role of covalence in the perovskite-type manganites [La,M(II)] MnO_3," Physical Review, October 15, 1955, 100, p. 564-573.

(32) WOLLAN, E. O. and KOEHLER, W. C.: "Neutron diffraction study of the magnetic properties of the series of perovskite-type compounds [(1-x)La,xCa] MnO_3," Physical Review, October 15, 1955, 100, p. 545-563.

(33) PRINCE, E.: "Crystal structures of two tetragonal pseudo-spinels," Bulletin of the American Physical Society, March 15, 1956, [2] 1, p. 132.

(34) BICKFORD, L. R., Jr.: "Ferromagnetic resonance absorption in magnetite single crystals," Physical Review, May 15, 1950, 78, p. 449-457.

(35) MENYUK, N.: "Stress effects in ferrites and generalization of switching coefficient for nonsquare materials," Lincoln Laboratory Memorandum M-2602, January 6, 1954.

(36) BROWN, D. R., BUCK, D. and MENYUK, N.: "A comparison of metals and ferrites for high-speed pulse operation," Transactions American Institute of Electrical Engineers (Communications and Electronics, 1955, No. 16, p. 631-634).

(37) BATES, L. F. and MARTIN, D. H.: "Domains of reverse magnetization," Proceedings Physical Society (London) February 1953, A66, p. 162-166; "Ferromagnetic domain nucleation in silicon iron," Proceedings Physical Society (London) February 1956, B69, p. 145-152.

(38) CHILDRESS, J. D.: "Memory-core heating by switching at high frequencies," Lincoln Laboratory Memorandum 6M-4137 (January 31, 1956).
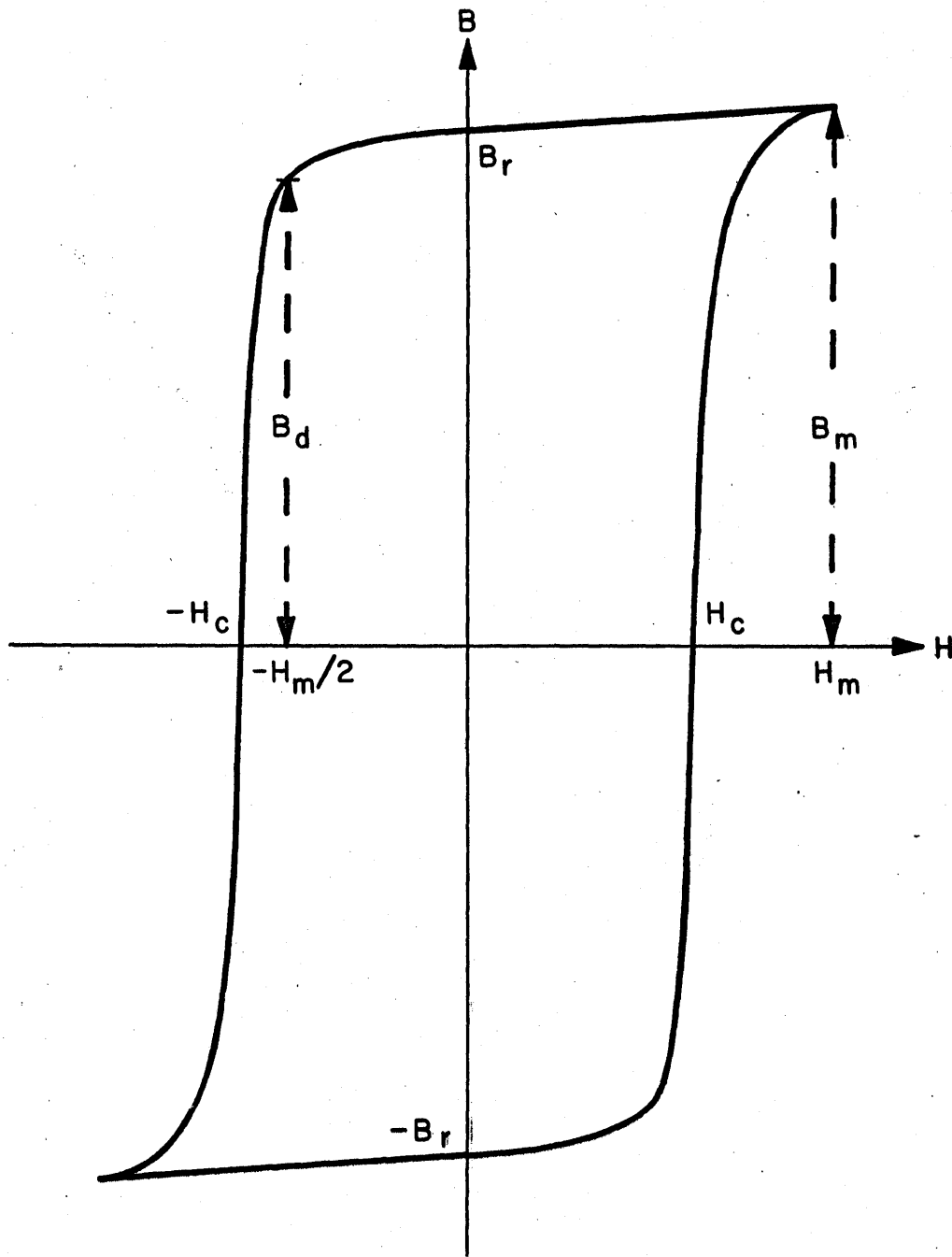
Fig. 1

Definition of terms determining the shape of the B-H loop.
At B_r information stored is a ONE, at $-B_r$ a ZERO. WRITE and
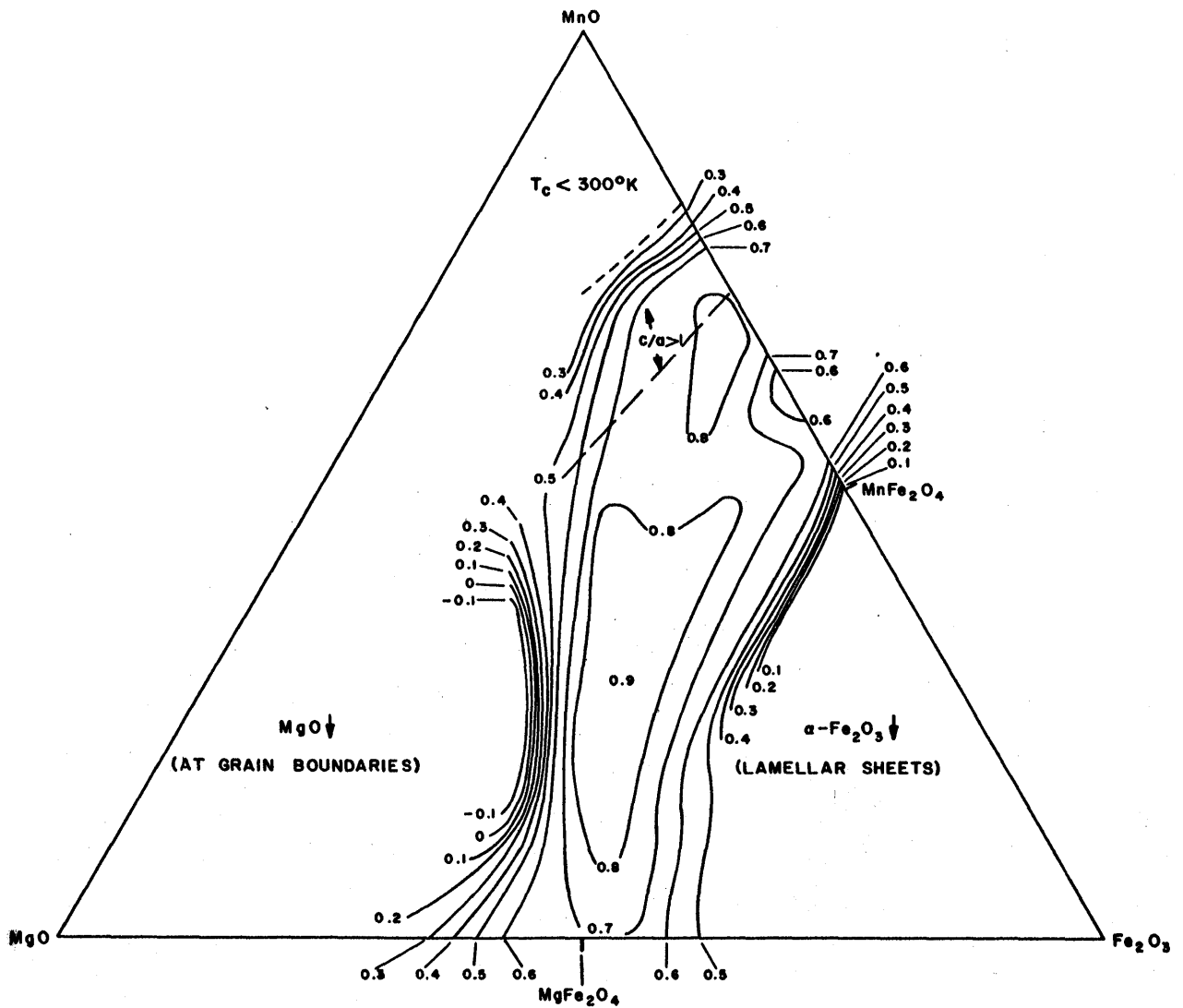READ pulses are H_m, $-H_m$.

Fig. 2

Room temperature contours of maximum squareness ratio in the as-mixed compositional system MgO-Fe₂O₃-MnO. Mixed oxides were fired in air between 1200°C and 1450°C; they were annealed for one hour in N₂ atmosphere at 1100°C. Squareness drops off sharply with precipitate formation and as curie temperature is approached. There is no discontinuity in squareness across boundary between cubic and tetragonal (c/a>1) spinels. Homogeneity observed to be important for squareness.
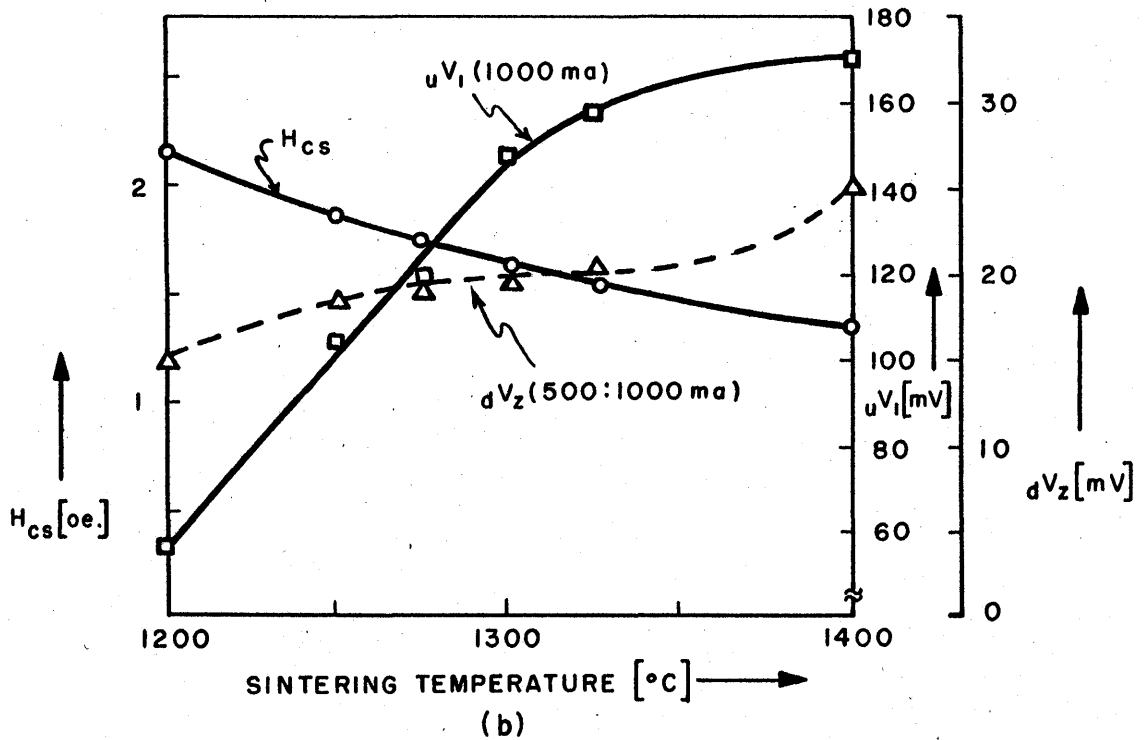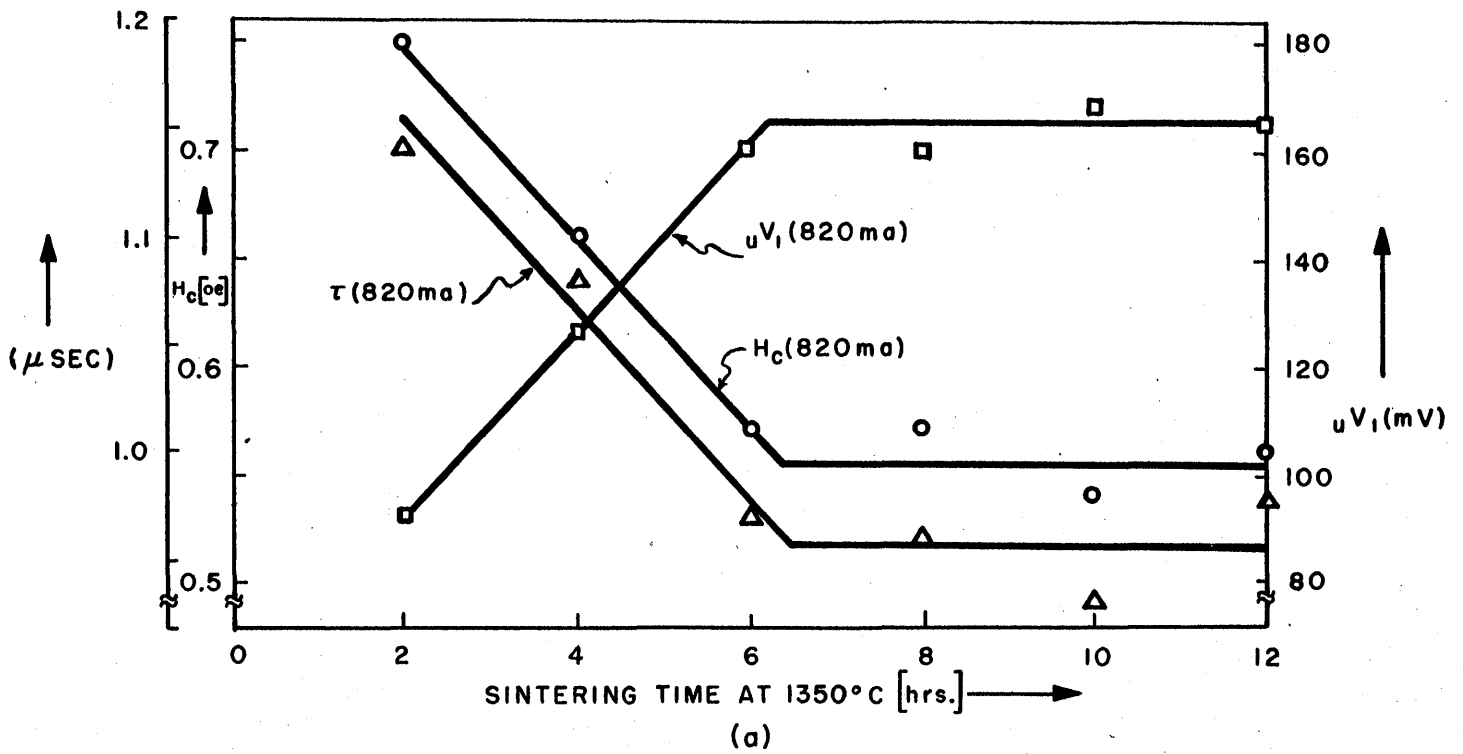
Fig. 3

Variations in switching time τ, coercivity H_c, noise voltage $_dV_z$, peak voltage signal $_uV_1$ caused by a read pulse on a memory core storing an undisturbed "one" with (a) sintering time at 1350°C and (b) temperature of 10 hr. sinter. If cores with $_uV_1 > 160$mV, $_dV_z < 25$mV with 1000 ma drive, 500 ma disturb currents are required, sintering temperature range throughout furnace must be 1330°C $< T < 1400$°C.
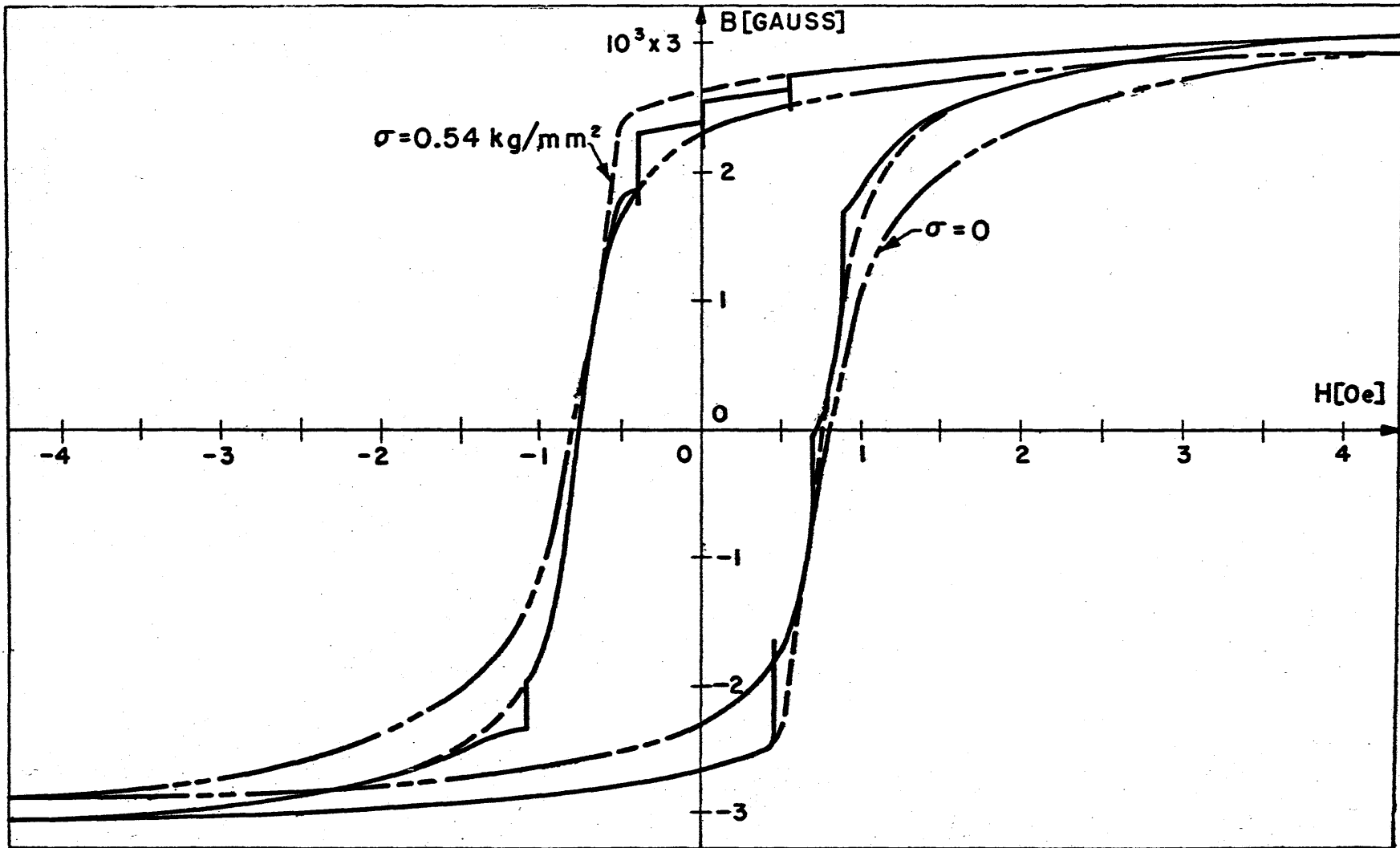
Fg. 4

Changes in loop shape of a core of ferroxcube 4-B with the application of an external compressive stress $\sigma = 0.54$ kg/mm². The stress was applied by loading a circumferential steel band with a weight. The solid hysteresis loop is that of a core under compression except when σ is removed and reapplied at certain field strengths. Detailed explanation of similar results for permalloy in terms of grain-boundary nucleation given in ref. (10).
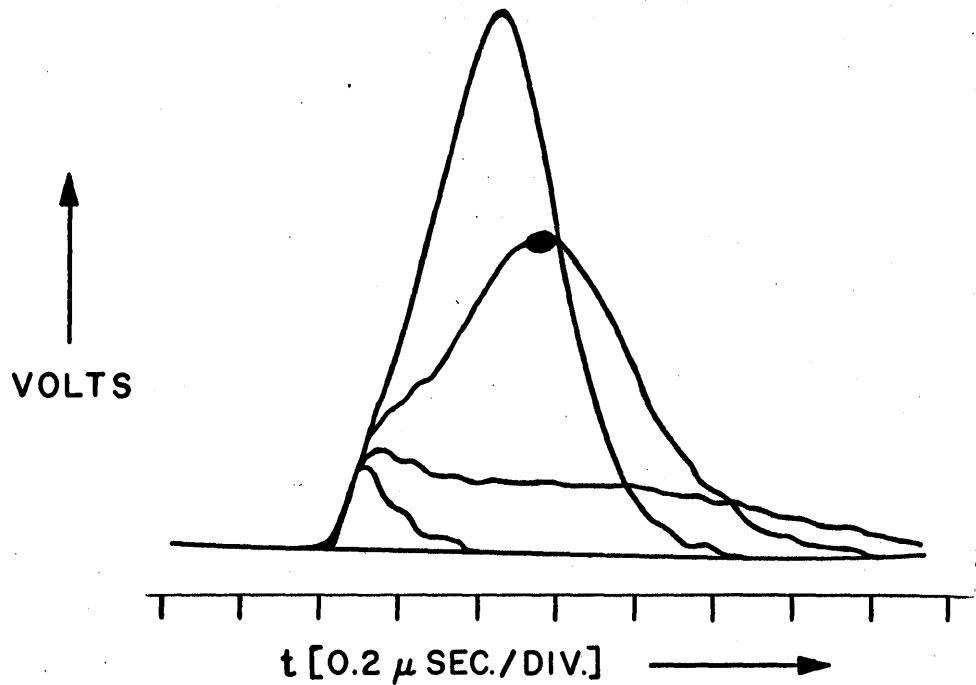
Fig. 5. Voltage-output wave forms for a magnesium-manganese memory core $(Mg_{0.8} Mn_{0.5} Fe_{1.7} O_4)$ driven by (1) a disturb read pulse $H_d = 1.1$ oe. (470 ma) which does not destroy the information stored, (2) a field which is low yet capable of destroying the stored information: $H = 1.4$ oe (575 ma), (3) minimum normal read pulse: $H_m = 1.8$ oe. (740 ma), and (4) maximum normal read pulse: $H_m = 2.1$ oe. (900 ma). The driving-pulse rise time is 0.2 μsec. The peak output voltages are 20, 30, 85, 140 mV, respectively. The dot at the peak of the normal read pulse marks the strobe time. In practice the output voltage is sampled at the time the signal-to-noise ratio is a maximum. Switching time is measured as the time the voltage is greater than 0.1 of the peak voltage.
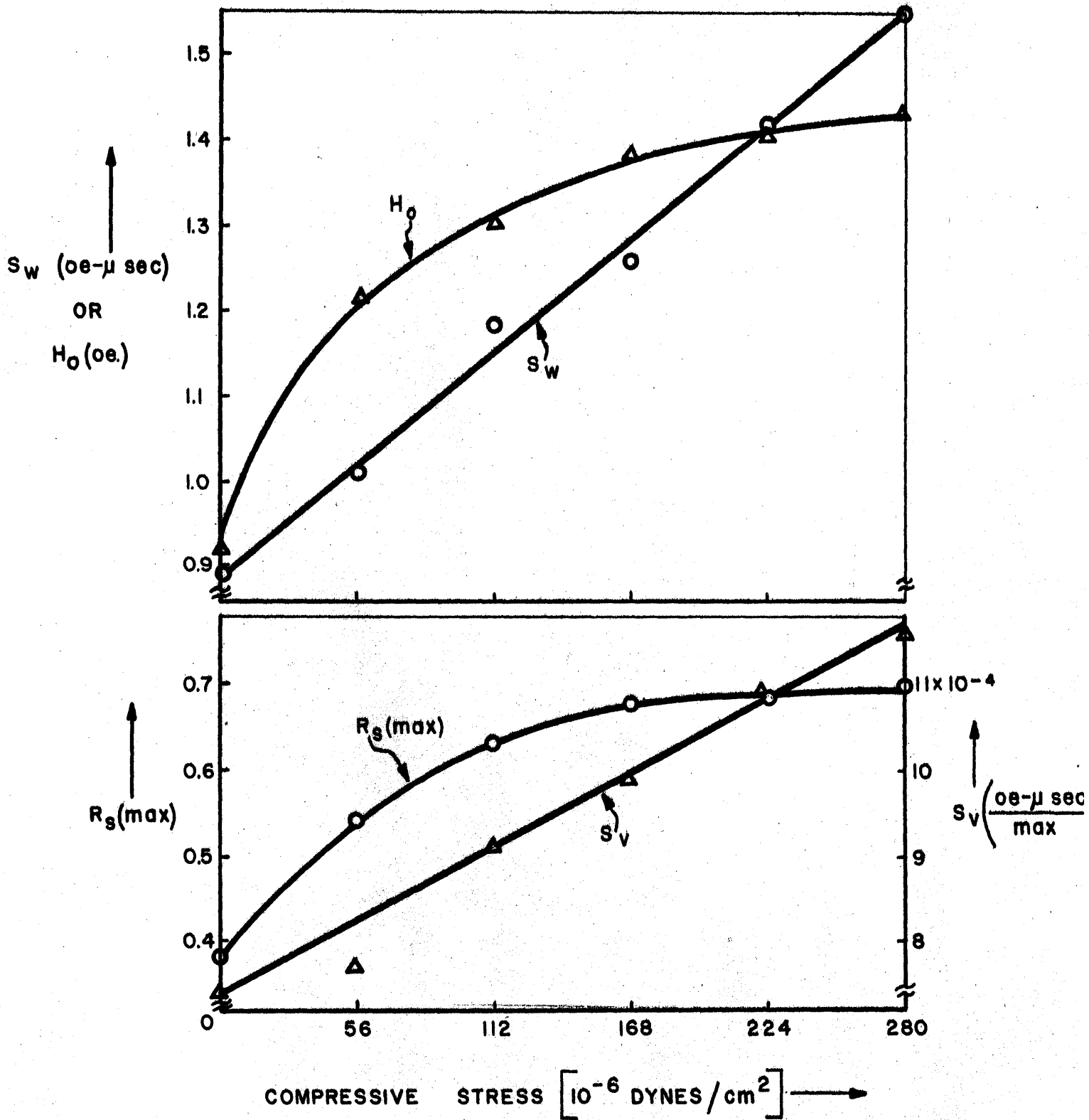
Fig. 6
Effect of compressive stress on several properties of a
Ferroxcube-103 core (after N Menyuk (35)). The switching coeffi-
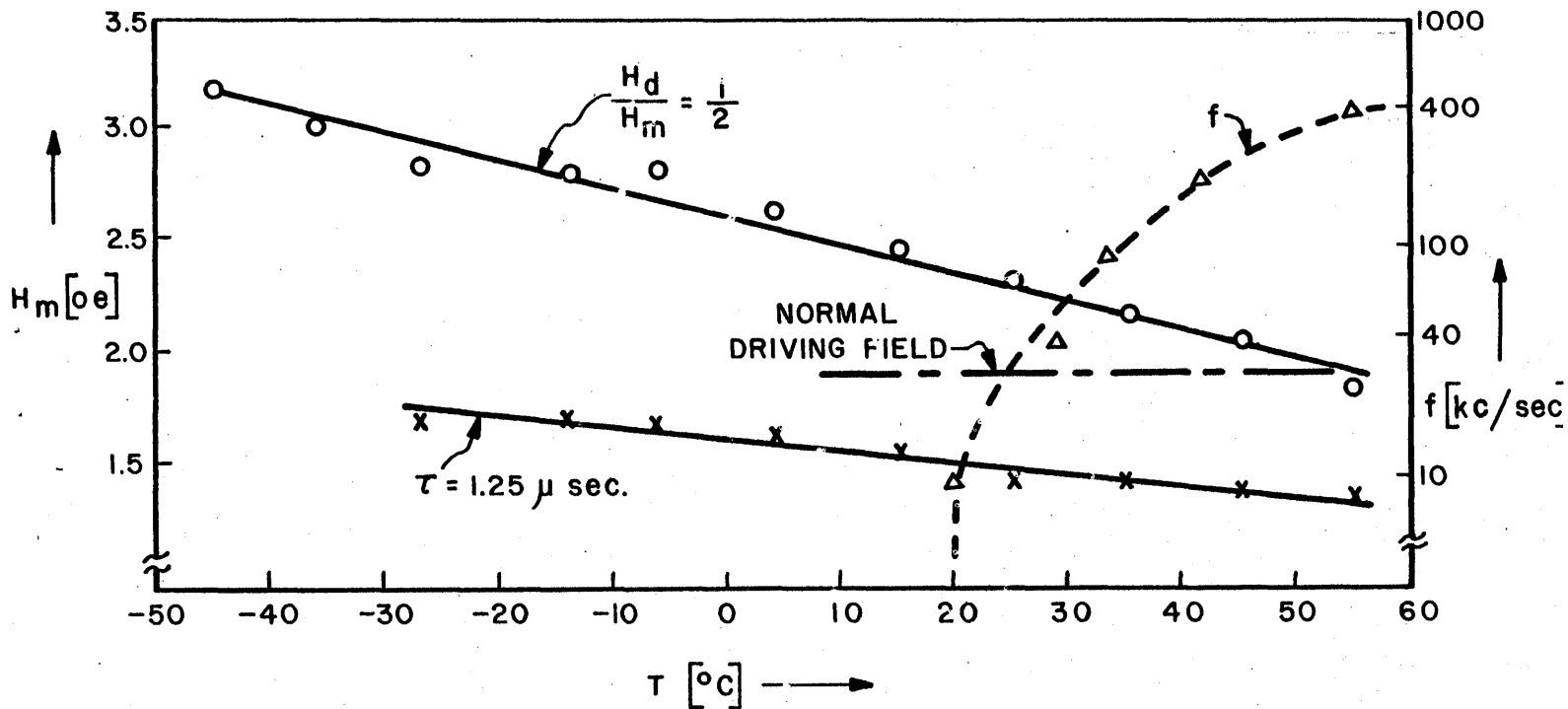cient S_w and threshold field H_o have been corrected for lack of
loop squareness.

$\dfrac{H_d}{H_m} = \dfrac{1}{2}$

$H_m [oe]$

f

NORMAL
DRIVING FIELD

$\tau = 1.25 \mu$ sec.

$f [kc/sec]$

3.5 — 1000

3.0 — 400

2.5 — 100

2.0 — 40

1.5 — 10

-50 -40 -30 -20 -10 0 10 20 30 40 50 60

$T [^\circ C] \longrightarrow$

Fig. 7

Temperature limitations for a $Mg_{0.8} Mn_{0.5} Fe_{1.7} O_4$ core used as a memory element in a two-to-one selection scheme (after J. Childress (38)). The switching time τ decreases with increasing maximum driving field H_m; the lower limit of satisfactory operation is $\tau = 1.25\mu sec$. For two-to-one selection, it is necessary to have $H_d/H_m > 0.5$, where H_d is the maximum disturb field which does not destroy the information contained in the core: the upper limit for satisfactory operation is therefore $H_d/H_m = 0.5$. These margins are plotted as a function of temperature along with the temperature of 50 juxtaposed cores immersed in a 20° C oil bath which are being switched with different repetition frequencies f. (In still air the rise in temperature with frequency is steeper: in actual operation the cores are separated from one another). The core temperature was determined indirectly by previously observing the switching characteristics as a function of temperature. The maximum possible frequency at which a core in a memory of $5\mu sec$ cycle time could be switched is 400 kc/sec. Current high-speed memories have $6\mu sec$ cycle time, and the cores are cooled by forced air.
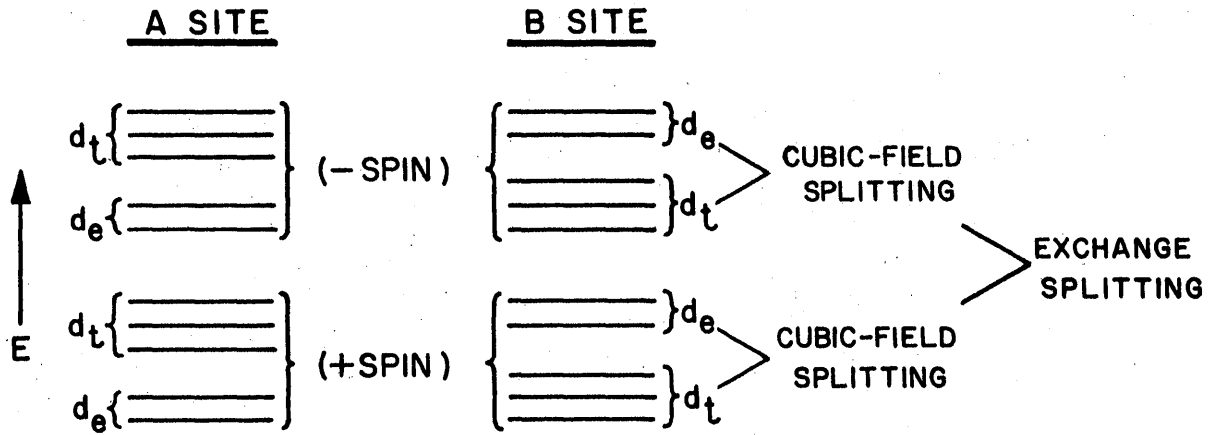
A-66145

FIG. 8

SCHEMATIC ENERGY LEVELS FOR d ORBITALS OF

CATIONS IN A OR B SITES OF A SPINEL−TYPE LATTICE

ANION

CATION 2   CATION 1

p_z p_y
p_x
p_x
p_y
p_z

(a)

CATION 2   ANION   CATION 1
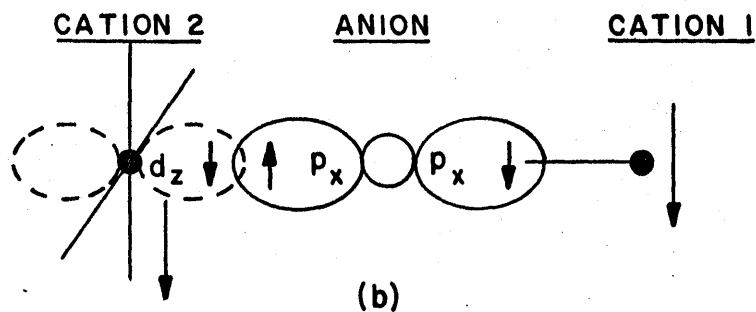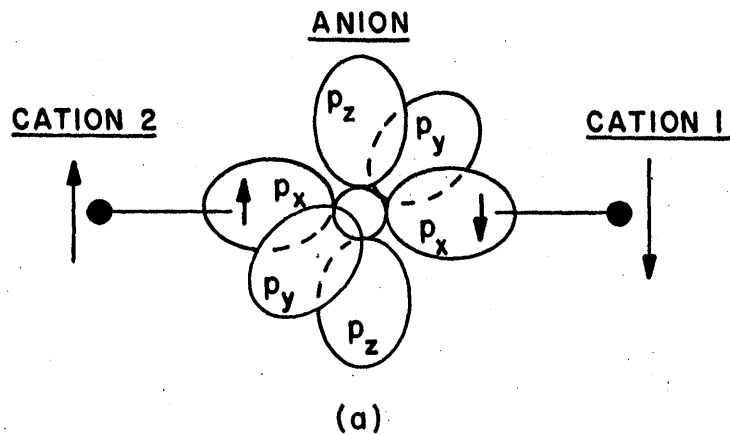
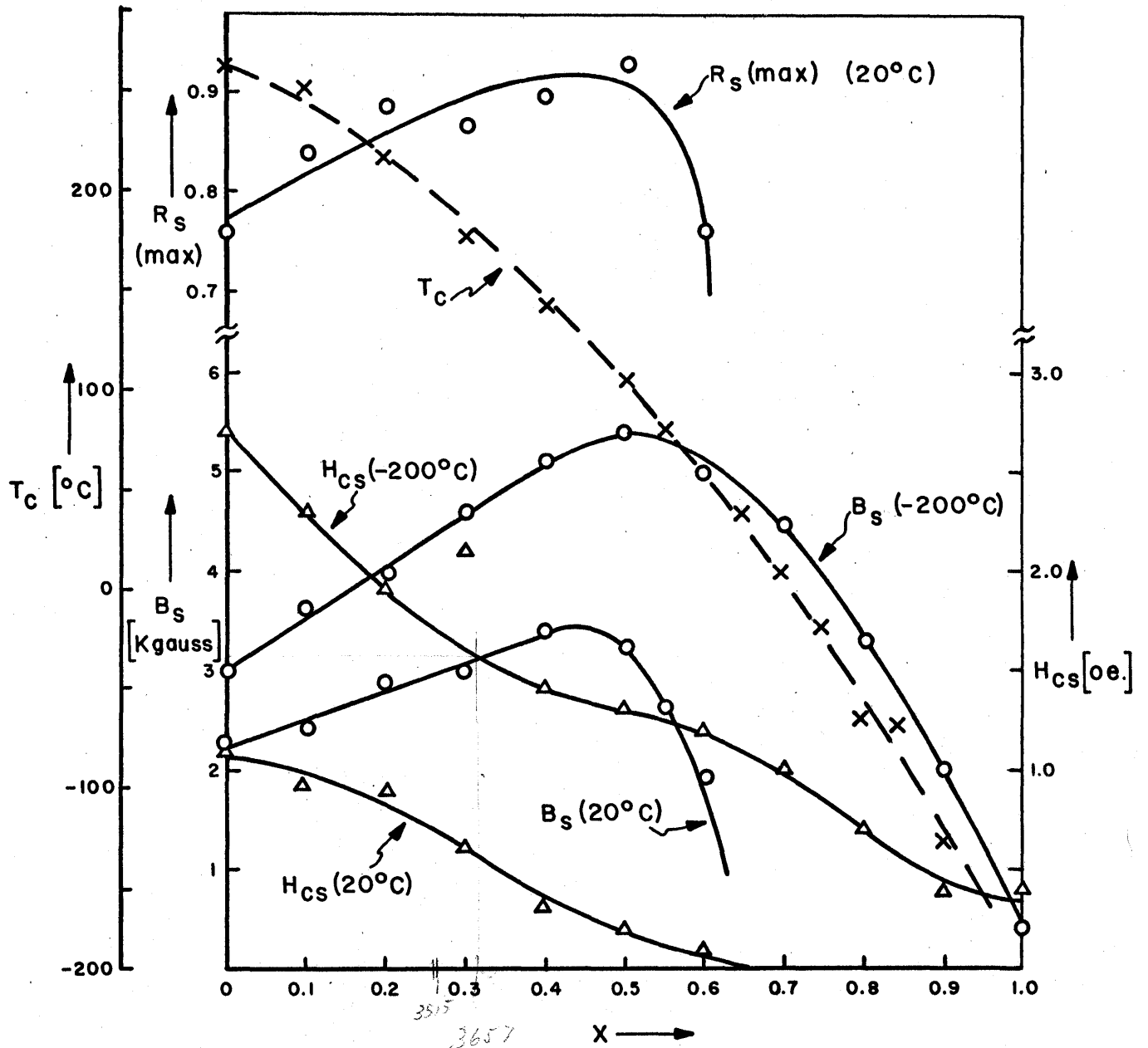d_z p_x p_x

(b)

FIG. 9

SCHEMATIC REPRESENTATION OF INDIRECT

SEMICOVALENT EXCHANGE:

(a) ANTIFERROMAGNETIC COUPLING

(b) FERROMAGNETIC COUPLING

A-66023

(a)

Fig. 10

Variation with x of Curie Temperature T_c, maximum squareness ratio R_s(max), saturation flux density (H_s= 30 oe.), and coercivity H_{cs} for the compositional series $(Mn_3O_4)_{0.15}$ $(MgFe_2O_4)_{0.85-x}$ $(ZnFe_2O_4)x$.